ANEXO III

SELECCIÓN POR EVALUACIÓN DE TÍTULOS, ANTECEDENTES Y OPOSICIÓN
DE PROFESORES QUE ASPIRAN A DESEMPEÑARSE
COMO PROVISIONALES Y/O SUPLENTES EN EL NIVEL TERCIARIO

DECLARACIÓN JURADA

DATOS PERSONALES

Apellido y Nombres: JUAN IGNACIO LABORDE TORRALLARDONA

Documento de Identidad: Tipo DNI 30.958.822

Lugar de nacimiento: LA PLATA

Fecha: 28/06/1984

Domicilio real: Calle 64 núm. 732, depto. E.

Localidad: LA PLATA

Partido: LA PLATA

Tel: 2216240740

Domicilio en el distrito de inscripción: Alsina 468, Pehuajó.

DESEMPEÑO ACTUAL

Se desempeña en cargo docente: **SI** Si la respuesta es afirmativa, indicar

Nivel: **SECUNDARIO y TERCIARIO**

Establecimiento: **EES DIEGEP n° 7245 “Colegio Jesus de Nazareth” / ISFDyT n° 74**

Distrito: GENERAL BELGRANO.

Cargo y/o área en que se desempeña:

- Profesor Suplente de **Matemática (MTM)** de 3° año de EES DIEGEP n° 7245 “Colegio Jesus de Nazareth” de General Belgrano.
  Desde Marzo 2019.
- Profesor Suplente de **Matemática de Ciclo Superior (MCS)** de 5° año de EES DIEGEP n° 7245 “Colegio Jesus de Nazareth” de General Belgrano.
  Desde Marzo 2021.

- Profesor Provisional de **Fisica y Elementos de Astronomía y Laboratorio II** de 2° año de Profesorado de Tercer Ciclo de la EGB y Educación Polimodal de Biología de ISFDyT n° 74 de General Belgrano.
  Desde Junio 2021.
- Profesor Provisional de **Historia de la Matemática** de 2° año de Profesorado de Tercer Ciclo de la EGB y Educación Polimodal de Matemática de ISFDyT n° 74 de General Belgrano.
  Desde Abril 2022.
- Profesor Provisional de **Fisica y Elementos de Astronomía y Laboratorio II** de 1° año de Profesorado de Tercer Ciclo de la EGB y Educación Polimodal de Química de ISFDyT n° 74 de General Belgrano.
  Desde Abril 2022.

ANTIGÜEDAD TOTAL EN LA DOCENCIA: 3 (dos) años y 8 (ocho) meses.

I. TÍTULOS Y ANTECEDENTES VALORADOS POR ARTÍCULO 60 DE LA LEY 10579 Y DECRETOS REGLAMENTARIOS

Evaluado por Listado 108: SI (tachar con X lo que no corresponda)

No será necesario para los docentes incorporados en los listados emitidos por la Dirección de Tribunales de Clasificación presentar documentación respaldatoria de los títulos y antecedentes comprendidos en dicha evaluación.

TÍTULO DOCENTE de la especialidad

En cada perspectiva o asignatura se consideran como títulos de la especialidad aquellos que figuran como habilitantes en el último Nomenclador de la Dirección General de Cultura y Educación.

Título: **Licenciatura en Física (en curso)**

Expedido por: **Facultad de Ciencias Exactas (UNLP)**

Fecha: **EN CURSO** Promedio de egreso: 8,00 (actual)

Título: **Profesorado de Física (en curso)**

Expedido por: **ISFD n°95 “Mary O. Graham” de La Plata**

Fecha: **EN CURSO** Promedio de egreso: 8,54 (actual)

ANTIGÜEDAD DOCENTE EN EL NIVEL TERCIARIO

Antigüedad en desempeño efectivo (rentado) en instituciones del nivel, con carácter de titular, provisional o suplente, al 31 de diciembre próximo pasado. Adjuntar comprobantes que permitan acreditar la antigüedad, institución y área de desempeño y clasificación del establecimiento en términos de desfavorabilidad.

Institución: ISFDyT n°74 (Gral. Belgrano) Dependiente de: DGCYE.

Clasificado como desfavorable: NO

Cargo y Área: Profesor Provisional de **Física y Elementos de Astronomía y Laboratorio I** de 1° año de Profesorado de Tercer Ciclo de la EGB y Educación Polimodal de Biología.
Desde: Junio 2020 Hasta: Abril 2021

Institución: ISFDyT n°74 (Gral. Belgrano) Dependiente de: DGCYE.

Clasificado como desfavorable: NO

Cargo y Área: Profesor Provisional de **Metodología de la Investigación Educativa en Matemática** de 4° año de Profesorado de Tercer Ciclo de la EGB y Educación Polimodal de Matemática.
Desde: Junio 2020 Hasta: Abril 2021

Institución: ISFDyT n°74 (Gral. Belgrano) Dependiente de: DGCYE.

Clasificado como desfavorable: NO

Cargo y Área: Profesor Provisional de **Física** de 4° año de Profesorado de Tercer Ciclo de la EGB y Educación Polimodal de Matemática.
Desde: Julio 2020 Hasta: Abril 2021

Institución: ISFDyT n°74 (Gral. Belgrano) Dependiente de: DGCYE.

Clasificado como desfavorable: NO

Cargo y Área: Profesor Provisional de **Topología** de 3° año de Profesorado de Tercer Ciclo de la EGB y Educación Polimodal de Matemática.
Desde: Mayo 2019 Hasta: Abril 2020

Institución: ISFDyT n°74 (Gral. Belgrano) Dependiente de: DGCYE.

Clasificado como desfavorable: NO

Cargo y Área Profesor Provisional de **Historia de la Matemática** de 3° año de Profesorado de Tercer Ciclo de la EGB y Educación Polimodal de Matemática.
Desde: Mayo 2019 Hasta: Abril 2020

.

ANTIGÜEDAD DOCENTE EN OTROS NIVELES

Antigüedad docente en establecimientos del nivel o modalidad a la que está dirigida la carrera : 3 (uno) años y 8 (ocho) meses.

Nivel o modalidad: **Secundario**
Cargo/ área: **Profesor suplente de Matemática de Ciclo Superior (MCS) de 5° año.**
Establecimiento: **EES DIEGEP n°7245 “Colegio Jesus de Nazareth” de Gral. Belgrano.**
Desde: 08/03/2021 Hasta: LA FECHA
Clasificado como desfavorable: NO

Nivel o modalidad: **Secundario**
Cargo/ área: **Profesor suplente de Matemática (MTM) de 3° año.**
Establecimiento: **EES DIEGEP n°7245 “Colegio Jesus de Nazareth” de Gral. Belgrano.**
Desde: 11/03/2019 Hasta: LA FECHA
Clasificado como desfavorable: NO

Nivel o modalidad: **Secundario Adultos**
Cargo/ área: **Profesor suplente de Matemática (MTM) de 1° año.**
Establecimiento: **EES CENS n°462 de La Plata.**
Desde: 24/09/2019 Hasta: 16/03/2020
Clasificado como desfavorable: NO

Nivel o modalidad: **Secundario**
Cargo/ área: **Profesor suplente de Matemática (MCS) de 4° año.**
Establecimiento: **EES n°65 “Pedro B. Palacios” de La Plata.**

Desde: 16/11/2018 Hasta: 15/04/2020
Clasificado como desfavorable: NO

Nivel o modalidad: **Secundario**
Cargo/ área: **Profesor suplente de Matemática (MAT) de 2° año.**
Establecimiento: **EES n°28 “Dante L. Segundo Pereira” de Villa Elisa, La Plata.**
Desde: 23/11/2018 Hasta: 13/12/2018
Clasificado como desfavorable: NO

Nivel o modalidad: **Secundario**
Cargo/ área: **Profesor suplente de Introducción a la Física (IAF) de 4° año.**
Establecimiento: **EES n°15 “Luis F. Leloir” de City Bell, La Plata.**
Desde: 24/10/2018 Hasta: 13/12/2018
Clasificado como desfavorable: NO

Nivel o modalidad: **Secundario**
Cargo/ área: **Profesor suplente de Matemática (MCS) de 4° año.**
Establecimiento: **EES n°31 “Gral. San Martin” de La Plata.**
Desde: 02/08/2018 Hasta: 22/10/2018
Clasificado como desfavorable: NO

Últimas dos calificaciones como profesor de Educación Superior:

Establecimiento ISFDYT n° 74 Gral. Belgrano **Dependiente de** DGCYE **Año** 2020 **Calificación obtenida:** 10 (diez).

Establecimiento ISFDYT n° 74 Gral. Belgrano **Dependiente de** DGCYE **Año** 2020 **Calificación obtenida:** 10 (diez).

OTROS TÍTULOS Y CERTIFICADOS BONIFICANTES (**NO CONSIGNA**)
Incluidos en el nomenclador vigente
Título **82. Enseñar Física con TIC 1 (Autoasistido)**

Expedido por **INFoD (Nuestra Escuela – Formación Docente Continua) - Curso aprobado por DI-2019-51-APN-INFD#MECCYT**

Fecha **19/07/2020**

Título **Plan Nacional Aprender Matemática en las Escuelas Bonaerenses**

Expedido por **ABC Campus Virtual – DGCyE INFoD (Nuestra Escuela – Formación Docente Continua)**

Fecha **07/12/2019**

II. OTROS TÍTULOS Y ANTECEDENTES VALORABLES PARA EL NIVEL TERCIARIO

Todos los aspirantes deberán presentar la documentación respaldatoria de los títulos y antecedentes que se consignen en este apartado.

POSTÍTULOS- POSTGRADOS (**NO CONSIGNA**)

Título...

.....Expedido por ....

Resolución N° .... Organismo que lo aprueba ....

OTROS TÍTULOS AFINES A LA ESPECIALIDAD QUE SE CONCURSA

EXPERIENCIA DOCENTE Y/O TÉCNICA EN LOS ÚLTIMOS 5 AÑOS

No incluir los antecedentes que hubieran sido detallados como antigüedad docente. Incluir breve caracterización de la tarea no docente.

- **Título:** DIPLOMATURA EN GESTIÓN DE ENERGÍAS RENOVABLES: SOLAR Y EÓLICA

  Expedido por: Universidad Nacional de Tres de Febrero (UNTREF Virtual) – Titulo en trámite.

  Descripción: Diplomatura emitida por la secretaria de Extensión de la UNTREF, iniciado en Junio 2018 y finalizado en Diciembre de 2018.

  Promedio Gral: 9,56.

- **Título:** Seminario "Project Management: Una práctica para gestionar proyectos de manera efectiva en las organizaciones"
  Expedido por: Universidad Nacional de La Plata (UNLP) – Facultad de Cs. Económicas - Secretaria de Posgrado.
  Descripción: Seminario de Posgrado en Cs. Económicas, dictado en Junio 2016. 12 horas de duración.

DICTADO DE CURSOS EN INSTITUCIONES RECONOCIDAS, EN LOS ÚLTIMOS CINCO AÑOS – Incluir sólo los cursos de la especialidad, con una duración mínima de 30 horas cátedra:
(**NO CONSIGNA**)
....
....
.

CONCURSOS DE OPOSICIÓN GANADOS EN EL NIVEL TERCIARIO

1. En el sistema educativo provincial
2. En otras instituciones terciarias no universitarias
3. En universidades nacionales o privadas

- **Establecimiento** ISFDyT n°74 (Gral. Belgrano) **Cargo** Profesor Provisional **Especialidad** Física y Elementos de Astronomía y Laboratorio 1 **Fecha** Marzo 2020
- **Establecimiento** ISFDyT n°74 (Gral. Belgrano) **Cargo** Profesor Provisional **Especialidad** Metodología de la Investigación Educativa en Matemática **Fecha** Marzo 2020
- **Establecimiento** ISFDyT n°74 (Gral. Belgrano) **Cargo** Profesor Provisional **Especialidad** Física **Fecha** Marzo 2020
- **Establecimiento** ISFDyT n°74 (Gral. Belgrano) **Cargo** Profesor Provisional **Especialidad** Topología **Fecha** Diciembre 2019
- **Establecimiento** ISFDyT n°74 (Gral. Belgrano) **Cargo** Profesor Provisional **Especialidad** Historia de la Matemática **Fecha** Diciembre 2019

INVESTIGACIONES, OBRAS Y PUBLICACIONES

Relacionadas con el área, asignatura y/o especialidad u otras afines o de índole pedagógica. Indicar los datos de publicación que permitan su localización. Se adjuntará una síntesis de cada trabajo editado o no.

- **“Ab initio study of F-centres in alkali halides”**
  (J. Hoya, J. I. Laborde, D. Richard, and M. Rentería)
  Computational Materials Science – Volume 139, 2017, Pages 1–7 - DOI: /10.1016/j.commatsci.2017.07.015
- **“Mechanical milled Zn-based semiconductors powders for photovoltaic devices”**
  (J.I. Laborde, J. Hoya, M.D. Reyes Tolosa, M.A. Hernandez-Fenollosa, L.C. Damonte)
  International Journal of Hydrogen Energy - Volume 39, Issue 16, 2014, Pages 8697-8701 - DOI: /10.1016/j.ijhydene.2013.12.051
- **-“Structural characterization of mechanical milled ZnSe and ZnTe powders for photovoltaic devices”**
  (J. Hoya, J. I. Laborde and L. C. Damonte)
  International Journal of Hydrogen Energy - Volume 37, Issue 19, 2012, Pages 14769-14772 - DOI: /10.1016/j.ijhydene.2011.12.082.

ACTIVIDADES DE ACTUALIZACIÓN Y PERFECCIONAMIENTO DOCENTE Y/O PROFESIONAL realizados en Instituciones reconocidas en los últimos 5 años.

- **Jornada Institucional – EES DIEGEP n°7245 “Colegio Jesus de Nazareth” de Gral. Belgrano.**
  Tema: Lectura y Escritura en Secundaria Y Conflictos y Ambiente Escolar.
  28 de Febrero de 2020
  Carga Horaria: 4 horas.

- **Jornada Institucional – ISFDyT n°74 de Gral. Belgrano.**
  Tema: Lectura y Escritura en Nivel Terciario.
  26 de Febrero de 2020
  Carga Horaria: 2 horas.

- **Jornada Institucional – EES n°31 “Gral. San Martin” de La Plata.**
  Tema: Ambiente Educativo.
  29 de Agosto de 2018
  Carga Horaria: 4 horas.

ASISTENCIA Y PARTICIPACIÓN EN CONGRESOS, SEMINARIOS, CONFERENCIAS ETC. sobre temáticas afines a la especialidad que se concursa.

- **“Polvos Nanoestructurados basados en ZN obtenidos por molienda mecánica para dispositivos fotovoltaicos”**
(J.I. Laborde, J. Hoya, L.C. Damonte)
AFA 2014 - 99a Reunión Nacional de Física de la Asociación Física Argentina – 22 al 25 de septiembre de 2014 – Tandil, Buenos Aires, Argentina. Con referato y publicación en acta.

- **“Mechanical milled doped Zn-based semiconductors powders for photovoltaic devices”**
(J.I. Laborde, J. Hoya, M. D. Reyes Tolosa, M.A. Hernandez-Fenollosa y L.C. Damonte)
UNLP 2013 – DEPARTAMENTO DE FISICA – Primer Jornada de Difusión de la Física Platense - 29 de noviembre de 2013 – La Plata, Buenos Aires, Argentina. Con publicación en acta.
- **“Structural characterization of mechanical milled ZnSe and ZnTe powders for photovoltaic devices”**
(J. Hoya, J.I. Laborde y L.C. Damonte)
UNLP 2013 – DEPARTAMENTO DE FISICA – Primer Jornada de Difusión de la Física Platense - 29 de noviembre de 2013 – La Plata, Buenos Aires, Argentina. Con publicación en acta.
- **“Mechanical milled doped Zn-based semiconductors powders for photovoltaic devices”**
(J.I. Laborde, J. Hoya, M. D. Reyes Tolosa, M.A. Hernandez-Fenollosa y L.C. Damonte)
HYFUSEN 2013 – 5to Congreso Nacional, 4to Congreso Iberoamericano. Hidrógeno y Fuentes Sustentables de Energía – 10 al 14 de junio de 2013 – Córdoba, Argentina, Con referato y publicación en acta.
- **“Impurity Atoms in Electrodeposited Films And Milled Powders of ZnMO (M=Co, Mn)”**
(J. Hoya, J.I. Laborde, M. Meyer, L.C. Damonte y L. Mendoza Zélis)
RAU 2013 - 23a Reunião Anual de Usuários (RAU) do Laboratório Nacional de Luz Sincrotron – 26 al 27 de febrero de 2013 – Campinas, SP, Brazil. Con referato y publicación en acta.

- **“Impurity Atoms in Electrodeposited Films And Milled Powders of ZnMO (M=Co, Mn)”**
(J. Hoya, J.I. Laborde, M. Meyer, L.C. Damonte y L. Mendoza Zélis)
NANOMAT 2012 – The 5th Latin American Conference on Metastable and Nanostructured Materials - 30 de septiembre al 2 de octubre de 2012 – Sao Carlos, SP, Brazil. Con referato y publicación en acta.
- **“Structural characterization of mechanical milled ZnSe and ZnTe powders for photovoltaic devices”**
(J. Hoya, J.I. Laborde y L.C. Damonte)
HYFUSEN 2011– 4to Congreso Nacional, 3er Congreso Iberoamericano. Hidrógeno y Fuentes Sustentables de Energía – 6 al 9 de junio de 2011 – Mar del Plata, Buenos Aires, Argentina. Con referato y publicación en acta.

- **“PALS study and ab-initio calculations on mechanical milled ZnSe and ZnTe powders”**
  (J. Hoya, J.I. Laborde y L.C. Damonte)
  HK2010 - Humboldt Kolleg – International Conference on Physics – 27 al 31 de marzo de 2011 – La Plata, Buenos Aires, Argentina. Con referato y publicación en acta.
- **“Ab-initio study of F-centers in alcali halides”**
  (J. Hoya, J.I. Laborde, D. Richard y M. Rentería)
  HK2010 - Humboldt Kolleg – International Conference on Physics – 27 al 31 de marzo de 2011 – La Plata, Buenos Aires, Argentina. Con referato y publicación en acta.
- **“Ab-initio study of F-centers in alcali halides”**
  (J. Hoya, J.I. Laborde, D. Richard y M. Rentería)
  FCM 2010 – At the Frontiers of Condensed Matter V – 6 al 10 de diciembre de 2010 – Buenos Aires, Argentina. Con referato y publicación en acta.
- **“Cálculos de primeros principios aplicados al estudio de las energías de absorción UV-visible de centros F en haluros alcalinos”**
  (J. Hoya, J.I. Laborde, D. Richard y M. Rentería)
  AFA 2010 - 95a Reunión Nacional de Física de la Asociación Física Argentina - 28 de septiembre al 1 de octubre de 2010 – Malargüe, Mendoza, Argentina. Con referato y publicación en acta.

DESARROLLO DE PROYECTOS Y/O EXPERIENCIAS RELACIONADOS CON EL NIVEL Y/O LA ESPECIALIDAD

- **Estadías en laboratorios: “Mechanical milled doped Zn-based semiconductors powders for photovoltaic devices”**
  Laboratorio Nacional de Luz Sincrotrón – Campinas, Sao Paulo, Brazil.
  Directora: Dra. Laura C. Damonte (UNLP) – 27 al 31 de marzo de 2012 y 19 al 22 de septiembre de 2012.

DISTINCIONES, PREMIOS Y BECAS (**No consigna**)

PARTICIPACIÓN EN JURADOS EVALUATORIOS DE ASIGNATURAS DE LA ESPECIALIDAD. (**No consigna**)

OTROS ANTECEDENTES que, a juicio del aspirante, puedan contribuir a una mejor información sobre su competencia en el área, asignatura y/o especialidad. (**No consigna**)

……………………………………………………………………………………………………….

En todos los casos se adjuntará copia de la documentación que certifique lo declarado.

LOS DATOS CONSIGNADOS TIENEN CARÁCTER DE DECLARACIÓN JURADA

Quien suscribe: JUAN IGNACIO LABORDE TORRALLARDONA, DNI Nº: 30.958.822, SOLICITA A Ud. ser inscripto /a en la cobertura de CARGOS DOCENTES.
DOMICILIO para NOTIFICACIONES: Calle 64 núm 732, depto. E, La Plata.

A la presente adjunto la declaración jurada que se indica en la Resolución N° 5886/03 con la documentación respaldatoria correspondiente.

Me notifico y declaro estar en conocimiento de la Res. 5848/02, Res. 1234/03 y Res. 5886/03 en todos sus términos, como así también de la nómina de los integrantes de la comisión evaluadora, los objetivos y /o expectativas de logro y los contenidos mínimos de la cátedra a cubrir, así como los requerimientos especiales consignados y cronograma.

Lugar y fecha......**La Plata, 11/03/21**..

Firma del aspirante .... LABORDE.

Recibió:

Lugar y fecha..Son .... folios.

Firma y sello de la autoridad interviniente

....

DIRECCIÓN GENERAL DE ESCUELAS Y CULTURA
DIRECCIÓN PROVINCIAL DE EDUCACIÓN SUPERIOR
UNIDAD ACADÉMICA
ESCUELA NORMAL SUPERIOR N° 1 "MARY O GRAHAM"
REGIÓN I-LA PLATA

La Dirección de la Escuela Normal Superior N° 1 - ISFD N° 95, deja constancia que **LABORDE JUAN IGNACIO** DNI: **30.958.822,** cursó y aprobó las siguientes áreas, espacios o perspectivas correspondientes al **Profesorado de Educación Secundaria en FÍSICA**. Manteniendo hasta la fecha condición de **Alumno Regular**.

LIBRO XII F 01

PRIMER AÑO	En Nros.	En letras	Fecha
Perspectiva Filosófico –Pedagógica I	8	ocho	21/11/2019
Perspectiva Pedagógica- Didáctica I	4	cuatro	18/08/2020
Perspectiva Socio-Política	8	ocho	19/11/2019
Psicología y Cultura en la Educación	7	siete	12/08/2020
Física y Elementos de Astronomía y Laboratorio I	10	diez	31/05/2019
Química y Laboratorio I	5	cinco	31/05/2019
Biología y Laboratorio I	7	siete	17/12/2019
Matemática Instrumental I	7	siete	31/05/2019
Integración Areal I	9	nueve	25/11/2019
Espacio de la Práctica Docente I	10	diez	20/11/2019
SEGUNDO AÑO			
Perspectiva Filosófico Pedagógica II	10	diez	27/11/2020
Perspectiva Pedagógico- Didáctica II	8	ocho	27/11/2020
Psicología y Cultura del Alumno de EGB 3 y Polimodal	9	nueve	27/11/2020
Física y Elementos de Astronomía y Laboratorio II	10	diez	Equiv. 27/11/2020
Química y Laboratorio II	9	nueve	11/12/2020
Biología y Laboratorio II	9	nueve	02/12/2020
Ciencias de la Tierra	8	ocho	25/02/2021
Matemática Instrumental II	7	siete	Equiv. 27/11/2020
Integración Areal II	9	nueve	22/03/2021
Espacio de la Práctica Docente II	9	nueve	27/11/2020
TERCER AÑO			
Perspectiva Filosófico Pedagógica Didáctica	-----	Adeuda	----------
Perspectiva Político Institucional	9	nueve	02/12/2021
Fuerzas, Movimiento y Energía mecánica y Laboratorio	C.A.	2021	----------
Ondas y Óptica Física y Laboratorio	10	diez	Equiv. 09/08/2019
Electromagnetismo y Termodinámica, y Laboratorio	10	diez	26/11/2021
Astronomía I	-----	Adeuda	----------
Cs Naturales y su Enseñanza	8	ocho	26/11/2021
Matemática Aplicada	10	diez	06/12/2021
Química y Laboratorio III	9	nueve	26/11/2021
E.D.I.	-----	Adeuda	----------
Espacio de la Práctica Docente III	-----	Adeuda	----------
CUARTO AÑO			
Física Moderna y Laboratorio	10	diez	Equiv. 09/08/2019
Física Teórica	10	diez	Equiv. 09/08/2019
Epistemología e Historia de la Física	-----	-----	----------
Astronomía II	-----	-----	----------
Taller de Física	-----	-----	----------
Física y su Enseñanza	-----	-----	----------
Matemática para Físicos y sus aplicaciones	-----	-----	----------
E:D:I	-----	-----	----------
Espacio de la Práctica Docente IV	-----	-----	----------
PORCENTAJE DE MATERIAS APROBADAS	**70,0%**		

Se extiende la presente en **La Plata** a los **14** días del mes de **febrero** de **2022**, para ser presentado ante las autoridades que correspondan.

Prof. MIRIAM B. CASTELLANO
Secretaria Unidad Académica
Escuela Normal Superior Nº 1
"Mary O. Graham"

Universidad Nacional de La Plata
Facultad de Ciencias Exactas

Historia Académica

Alumno: JUAN IGNACIO LABORDE
Legajo: 49144/4
Carrera: Licenciatura en Física
Plan: 1988

Fecha	Materia	Tipo	Nota	Resultado
04/07/2014	MATEMATICAS ESPECIALES I (S0203)	Examen	7 (Siete)	Aprobado
26/03/2014	MECANICA ANALITICA (S0205)	Examen	2 (Dos)	Reprobado
21/10/2013	ANALISIS DE SEÑALES (O0310)	Examen	10 (Diez)	Aprobado
17/04/2013	ANALISIS MATEMATICO II (E0203)	Examen	5 (Cinco)	Aprobado
29/08/2012	FISICA MACROSCOPICA (S0204)	Examen	5 (Cinco)	Aprobado
14/03/2012	SEMINARIOS DE FISICA DEL SOLIDO (O0258)	Cursada		Regular
05/03/2012	SIMUL. COMPUT. EN FISICA DEL SOLIDO Y MEC. ES. (O0282)	Cursada		Abandonó
22/12/2011	SEMINARIOS DE FISICA DE PARTICULAS Y CAMPO (O0260)	Cursada		Regular
14/12/2011	FISICA GENERAL IV (S0201)	Examen	10 (Diez)	Aprobado
14/12/2011	FISICA EXPERIMENTAL IV (S0202)	Examen	7 (Siete)	Aprobado
20/08/2011	ELECTRONICA (O0246)	Cursada		Regular
16/08/2011	MECANICA ANALITICA (S0205)	Cursada		Regular
31/12/2010	MECANICA ESTADISTICA (S0213)	Cursada		Regular
31/12/2010	ALGEBRA LINEAL: APLICACIONES FISICAS (O0292)	Cursada		Regular
31/12/2010	MECANICA CUANTICA II (S0211)	Cursada		Regular
31/12/2010	EXPERIMENTOS CUANTICOS II (S0212)	Cursada		Regular
31/12/2010	ALGEBRA LINEAL (O0253)	Cursada		Abandonó
31/12/2009	ELECTROMAGNETISMO (S0207)	Cursada		Regular
31/12/2009	EXPERIMENTOS CUANTICOS I (S0210)	Cursada		Regular
31/12/2009	ANALISIS DE SEÑALES (O0310)	Cursada		Regular
31/12/2009	MECANICA CUANTICA I (S0209)	Cursada		Regular
31/12/2009	MATEMATICAS ESPECIALES II (S0206)	Cursada		Regular
22/12/2009	FISICA GENERAL III (E0208)	Examen	8 (Ocho)	Aprobado
24/11/2009	FISICA EXPERIMENTAL III (E0209)	Examen	9 (Nueve)	Aprobado
31/12/2008	MATEMATICAS ESPECIALES II (S0206)	Cursada		Abandonó
31/12/2008	EXPERIMENTOS ELECTROMAGNETICOS (S0208)	Cursada		Regular
31/12/2008	ELECTROMAGNETISMO (S0207)	Cursada		Abandonó

Historia Académica

Alumno: JUAN IGNACIO LABORDE
Legajo: 49144/4
Carrera: Licenciatura en Física
Plan: 1988

Fecha	Materia	Tipo	Nota	Resultado
31/12/2007	MATEMATICAS ESPECIALES I (S0203)	Cursada		Regular
06/09/2007	FISICA GENERAL II (E0206)	Examen	7 (Siete)	Aprobado
26/06/2007	ANALISIS MATEMATICO I (E0201)	Examen	9 (Nueve)	Aprobado
31/12/2006	ANALISIS MATEMATICO II (E0203)	Cursada		Regular
31/12/2006	MATEMATICAS ESPECIALES I (S0203)	Cursada		Abandonó
28/11/2006	ANALISIS MATEMATICO I (E0201)	Examen	2 (Dos)	Reprobado
27/06/2006	FISICA EXPERIMENTAL II (E0207)	Examen	9 (Nueve)	Aprobado
09/05/2006	ALGEBRA (E0202)	Examen	9 (Nueve)	Aprobado
31/12/2005	FISICA GENERAL IV (S0201)	Cursada		Regular
31/12/2005	FISICA EXPERIMENTAL IV (S0202)	Cursada		Regular
30/03/2005	FISICA GENERAL I (E0204)	Examen	8 (Ocho)	Aprobado
31/12/2004	FISICA EXPERIMENTAL III (E0209)	Cursada		Regular
31/12/2004	ALGEBRA (E0202)	Cursada		Regular
31/12/2004	FISICA GENERAL III (E0208)	Cursada		Regular
31/12/2004	FISICA MACROSCOPICA (S0204)	Cursada		Regular
31/12/2003	ANALISIS MATEMATICO I (E0201)	Cursada		Regular
31/12/2003	FISICA GENERAL II (E0206)	Cursada		Regular
31/12/2003	ALGEBRA (E0202)	Cursada		Abandonó
02/12/2003	FISICA EXPERIMENTAL I (E0205)	Examen	9 (Nueve)	Aprobado
31/12/2002	FISICA GENERAL II (E0206)	Cursada		Abandonó
31/12/2002	ANALISIS MATEMATICO I (E0201)	Cursada		Abandonó
31/12/2002	FISICA EXPERIMENTAL I (E0205)	Cursada		Regular
31/12/2002	FISICA GENERAL I (E0204)	Cursada		Regular
31/12/2002	FISICA EXPERIMENTAL II (E0207)	Cursada		Regular
31/12/2002	ALGEBRA (E0202)	Cursada		Abandonó

Promedios
Título: **Licenciado en Física**
Promedio con aplazos: 7.25

Historia Académica

Alumno: JUAN IGNACIO LABORDE
Legajo: 49144/4
Carrera: Licenciatura en Física
Plan: 1988

Promedio sin aplazos: 8.00

Porcentaje de Aprobación
Título: **Licenciado en Física**
Plan Básico: 53.00%

UNIVERSIDAD
NACIONAL
DE LA PLATA

Universidad Nacional de La Plata

Facultad de Ciencias Exactas

Certificado de Alumno Regular

Facultad de Ciencias Exactas certifica que el alumno JUAN IGNACIO LABORDE con legajo número 49144/4, DNI 30958822, de origen Argentina, se encuentra actualmente regular en la carrera de Licenciatura en Física, plan 1988, con año de ingreso 2002.

A su pedido y para ser presentado ante quien corresponda se extiende el presente en la ciudad de La Plata, a los 11 días del mes de marzo de 2022.

CÓDIGO DE VALIDACIÓN:

22031114565656

Este certificado podrá ser validado ingresando a: **https://www.guarani-exactas.unlp.edu.ar/validador_certificados** y completando con el código de validación que aparece arriba entre asteriscos (*), o bien escaneando el código QR que aparece en pantalla.

Este certificado estará vigente hasta la fecha Sin Vencimiento

Buenos Aires
Provincia

DESIGNACION

Dirección General de Cultura y Educación
Secretaría de Asuntos Docentes La Plata

Sr./ a Director/ a Escuela N° ES N: 65 FECHA: 14/11/18

Comunico a Ud. que el/la docente LABORDE JUAN IGNACIO

CUIL: 2013095882214 LIST: 10815 VUELTA: 12 PJE: 10,60 PROMEDIO: —

INF IT 7

Ha sido designado ~~PROVISIONAL~~ / [✓ SUPLENTE] de Giulietti M.Laura CUIL 27/21308313/6

CUPOF	AREA / ASIGNATURA	CARGO / HS. / MOD.	AÑO / SECCIÓN	HORARIO					TURNO
				LUNES	MARTES	MIERCOLES	JUEVES	VIERNES	
148706	Matemática	3	4 A	/	7.30	/	/	7.30	M
					9.34			8.30	

MOTIVO DE AUSENCIA: Licencia Medio ID: 915830
(EN CASO DE LICENCIA MEDICA CONSIGNAR ID)

DESDE 12/11/18 HASTA 26/11/18 Enfermedades infectocontagiosas en la Escuela? SI - [✓ NO]

La Toma de Posesión se encuadra en la RES N° 331/18

Medios de Transporte: Oeste

Teléfono del Establecimiento: 221 15 6057425

Domicilio del Establecimiento: 28 e/ 35 y 36

Sandra Pastrana
S.P.O.T.
SAD II - LA PLATA

Digo 26/11/18

Sandra Pastrana
S.P.O.T
SAD II - LA PLATA

Es copia del original

Dipl. Pa[illegible] Bianchi
E.E.S. 65 - La Plata

SE EXTIENDE HASTA 28/2/18

Prof. Ruben Dario Seminario G
Vicedirector
EES N° 65
La Plata

Buenos Aires
Provincia

DESIGNACION

Dirección General de Cultura y Educación
Secretaría de Asuntos Docentes La Plata

Sr./ a Director/ a Escuela N° E.E.S.Nº28 FECHA: 21 | 11 | 18

Comunico a Ud. que el/la docente CABORDE JUAN IGNACIO
SNEME 347

CUIL: 20/30958822/4 LIST: 102 B VUELTA: PJE: 10,60 PROMEDIO —

Ha sido designado
PROVISIONAL - SUPLENTE de Mantovani Eliana CUIL: 27/26.593 628/ 2

CUPOF	AREA / ASIGNATURA	CARGO / HS. / MOD.	AÑO / SECCIÓN	HORARIO					TURNO
				LUNES	MARTES	MIERCOLES	JUEVES	VIERNES	
2141102	MATEMATICA	4 mod	2D	/	13^{30} a	/	/	15^{40} a	T
				/	15^{00}	/	/	17^{15}	

MOTIVO DE AUSENCIA: 5462 a

(EN CASO DE LICENCIA MEDICA CONSIGNAR ID)

DESDE 21/11/18 HASTA 12/12/18 Enfermedades Infectocontagiosas en la Escuela ? SI - NO

La Toma de Posesión se encuadra en la RES N° 331/18

Medios de Transporte: TALP - TREN - 273

Teléfono del Establecimiento : 473-1219

Domicilio del Establecimiento: 5 E/ 421 Y 422 - VILLA ELISA (SEDE)

SAD LA PLATA

CLAUDIA ALEJANDRA LEGONE
Secretaria
Escuela E.S. Nº 28
Villa Elisa

p. cop. orig.

Toma posesión 23/11/18.

CLAUDIA ALEJANDRA LEGONE
Secretaria
Escuela E.S. Nº 28
Villa Elisa

Buenos Aires
Provincia

irección General de Cultura y Educación
cretaría de Asuntos Docentes La Plata

DESIGNACION

María Cristina Galvan

FECHA: 22 | 10 | 18

r./ a Director/ a Escuela N° 15

omunico a Ud. que el/la docente LABORDE JUAN IGNACIO
[illegible] 247

UIL: 20-[illegible] 14 LIST: 2083 VUELTA: PJE: 11,13 PROMEDIO

Ha sido designado
PROVISIONAL - SUPLENTE de LUJAN PABLO CUIL: 20-18285157-15

CUPOF	AREA / ASIGNATURA	CARGO / HS. / MOD.	AÑO / SECCIÓN	HORARIO					TURNO
				LUNES	MARTES	MIERCOLES	JUEVES	VIERNES	
165244	IAF	2	4°E			10^{25} 12^{25}			T

OTIVO DE AUSENCIA: ID: 24F4F7
(EN CASO DE LICENCIA MEDICA CONSIGNAR ID)

ESDE 22/10/18 HASTA 7/11/18 Enfermedades Infectocontagiosas en la Escuela ? SI - NO

a Toma de Posesión se encuadra en la RES N° 331/18
edios de Transporte:
eléfono del Establecimiento :
omicilio del Establecimiento:

María Cristina Galvan

Por prolongación de la suplencia, el profesor LABORDE JUAN IGNACIO continúa en el cargo designado hasta el 13/12/18

Susana Herrero
Pro Secretaria
E.E.S. Nº 15

Vaccani Adriana
Directora
E.E.S. Nº 15

Buenos Aires
Provincia

Dirección General de Cultura y Educación
Secretaría de Asuntos Docentes La Plata

DESIGNACION

FECHA: 1 | 9 | 18

Sr./ a Director/ a Escuela N° EES 31

Comunico a Ud. que el/la docente LABORDE JUAN IGNACIO

1N FINC 117

CUIL: 20 130958822 14 LIST: 108 B VUELTA: PJE: 10,30 PROMEDIO —

Ha sido designado SUPLENTE de **HERRERO Marisa** CUIL: **27-12912833-5**

CUPOF	AREA / ASIGNATURA	CARGO / HS. / MOD.	AÑO / SECCIÓN	HORARIO					TURNO
				LUNES	MARTES	MIERCOLES	JUEVES	VIERNES	
1902845	MATEMATICA	3 mod	4º3ª			08:30	10:50		M
						09:30	12:50		

MOTIVO DE AUSENCIA: Lic. 114 a 3

(EN CASO DE LICENCIA MEDICA CONSIGNAR ID)

DESDE **30/07/2018** HASTA **28/07/2018** Enfermedades Infectocontagiosas en la Escuela ? **NO**

La Toma de Posesión se encuadra en la RES N° 331/18

Medios de Transporte: **TODOS AL CENTRO**

Teléfono del Establecimiento: **421-1372**

Domicilio del Establecimiento: **46 Nº 366**

Golvan
LA PLATA

desde 30/7/18 al
30/9/18

Liliana N. Díaz
Secretaria
E.E.S. Nº 31 L.P.

Prolong de suplencia 30/9/18 al 30/11/18

[illegible]
Secretaria
E.E.S. N° 31 La Plata

Ministerio de Educación
Argentina

INFoD
Instituto Nacional de Formación Docente

NUESTRA ESCUELA
FORMACIÓN DOCENTE CONTINUA

Segundo Trayecto 2017-2021
CERTIFICADO

Se hace constar que **Juan Ignacio Laborde** D.N.I. **30958822**, ha cursado y aprobado el día **26 de mayo de 2020** los contenidos formativos del curso **82. Enseñar Física con TIC I · Autoasistido** con una carga horaria total de **DIEZ** (**10**) horas reloj, perteneciente al **PROGRAMA NACIONAL DE FORMACIÓN PERMANENTE "NUESTRA ESCUELA"**, desarrollado por el Instituto Nacional de Formación Docente.

Se extiende el presente, sin raspaduras ni enmiendas, en la provincia de ***Buenos Aires****, República Argentina, a los 19 días del mes Julio de 2020.*

Dra. Mercedes del Valle Leal
DIRECTORA EJECUTIVA
Instituto Nacional de Formación Docente

Mg Claudia C. Bracchi
Subsecretaria de Educación
Dirección General de Cultura y Eduación
Provincia de Buenos Aires

Curso aprobado por DI-2019-51-APN-INFD#MECCYT

FDE-06-20-0268753

134f9c2ea93d23a6ecd0ab0dbfb3390bc3a37fd592da5b025832731de5388707

Computational Materials Science 139 (2017) 1–7

Contents lists available at ScienceDirect

Computational Materials Science

journal homepage: www.elsevier.com/locate/commatsci

Ab initio study of *F*-centers in alkali halides

J. Hoya [a,b], J.I. Laborde [a], D. Richard [a,b,*], M. Rentería [a,b]

[a] Departamento de Física, Facultad de Ciencias Exactas, Universidad Nacional de La Plata, CC 67, 1900 La Plata, Argentina
[b] Instituto de Física La Plata (IFLP, CCT La Plata, CONICET-UNLP), Facultad de Ciencias Exactas, Universidad Nacional de La Plata, CC 67, 1900 La Plata, Argentina

ARTICLE INFO

Article history:
Received 1 June 2017
Received in revised form 6 July 2017
Accepted 16 July 2017

Keywords:
Alkali halide
F-center
DFT
Ab initio
Defect level

ABSTRACT

The structural and electronic properties of an electron trapped at vacant anion site in alkali halides are investigated using first principles electronic structure calculations with the supercell method. In order to determine the spatial electronic charge density and band structure of the studied systems we used the Augmented Plane Waves plus local orbital (APW + lo) method in the framework of the Density Functional Theory (DFT), considering the Wu and Cohen parametrization of the generalized gradient approximation (WCGGA) for the exchange and correlation energy, and the modification of Tran and Blaha to the Becke and Johnson exchange potential (mBJ method). We discuss the improvements in the description of the defect levels induced by the vacancies using mBJ compared to WCGGA. Additionally, we revisit the experiment to perform a new determination of the UV/Vis absorption energies in *F*-centers. In the theoretical framework used, we demonstrate that the bound electron at the *F*-center is localized within a sphere with diameter twice the lattice parameter. From the comparison of our theoretical predictions with the Mollwo-Ivey relation that comes from this new experiment, we show that the mBJ method predicts accurately the energy band gaps and gives better energy values for the *s*-*p* transitions that give rise to the optical absorption energies.

1. Introduction

The *F*-center is a lattice defect which consists of an electron bound at a vacant negative ion site. It is the simplest defect that can occur in ionic crystals like the alkali halides, when halogen vacancies are produced by, for example, X-ray irradiation [1,2]. In these cases, when an anion is removed from the host crystal, it is replaced by an electron that occupies a donor state of a_{1g}-like symmetry in the ground state (*s*-type state). The electronic transition to a defect-induced level of t_{1u} symmetry (*p*-type state) explains the optical absorption energy peaks observed for *F*-centers in UV–Vis absorption experiments. In this way, the fundamental optical absorption energies arise from electronic transitions from the lowest 1*s* to 2*p* bound levels, according to the dipole selection rule. Many experimental and theoretical efforts have been done from the very beginning to study *F*-centers [2,3]. More recently, many *ab initio* methods were used in order to predict structural and electronic properties of the anion vacancies in alkali halides [4–10]. However, the study of *F*-centers by first-principles goes beyond the rocksalt structure, and it has been applied to a wide variety of structures. Among them, we can find, for example, bulk calculations in fluorite [11–13], perovskite [14,15], rutile [16–18], and anastase [18] structures, which gave a description of the *F*-center with different degrees of success depending on the used *ab initio* approach.

In this work, the UV/VIS absorption experiment was revisited for a variety of alkali halides, and we present a systematic *ab initio* structural and electronic band structure study for the following compounds: KI, KBr, KCl, NaCl, LiCl, NaF, and LiF. To this purpose we used the WIEN2k implementation of the Augmented Plane Wave plus local orbitals (APW + lo) method, in the framework of the DFT [19]. For the exchange and correlation energy, we first considered the Wu and Cohen parametrization of the generalized gradient approximation (WCGGA) [20]. Because it is known that this approximation systematically subestimates the energy band gaps E_g for most semiconductors [21], we also used the modified version of the Becke and Johnson exchange potential proposed by Tran and Blaha (mBJ method), which gives very accurate values of E_g in most semiconductors and insulators [22–24]. For the alkali halides that are subject of this study, we analyze how the improvements in the prediction of the E_g energies using the mBJ method affect the position of the defect levels when halogen vacancies are produced, and how better the electronic band structure is correlated with the experimental optical response in *F*-centers. To our knowledge, this

---

[*] Corresponding author at: Instituto de Física La Plata (IFLP, CCT La Plata, CONICET-UNLP), Facultad de Ciencias Exactas, Universidad Nacional de La Plata, CC 67, 1900 La Plata, Argentina.

E-mail address: richard@fisica.unlp.edu.ar (D. Richard).

http://dx.doi.org/10.1016/j.commatsci.2017.07.015

is the first time the APW + lo method is systematically applied to the study of these systems in this way.

2. Experimental procedure

The *F*-centers in the samples were prepared by the method of ionizing radiation, using X-rays. Alkali halide single crystals were irradiated for about 5 min at room temperature and normal pressure using the X-ray tube (at 40 kV, 30 mA, with a rhodium anode) of a Philips Wavelength X-ray (fluorescence) spectrometer at YPF Technological Center (Ensenada, Argentina). The absorption spectra were measured at room temperature in air using a UV–Vis Cintra 20 double-beam spectrophotometer (GBC Scientific Equipment Ltd.), ranging from 300 to 850 nm in 0.427 nm steps, except for LiF, where the 190–900 nm range was used. The slit-width was set to 0.8 nm and both deuterium and tungsten-iodine lamps were used to cover this wavelength range. A Ho_2O_3 glass sample was previously used as wavelength standard for calibration of the spectrophotometer. In Fig. 1 we present the obtained spectra. For each compound, the absorption energy E_a was obtained from the corresponding spectrum by a Gaussian fitting after subtracting a linear background. The results for E_a are presented in Table 1 (fourth column) and plotted in Fig. 2. These measured values are in very good agreement with those reported by other authors [2]. According to our results, we obtained the empirical Mollwo-Ivey relation:

$$E_a(d) = 16.5(9)d^{-1.76(6)} \tag{1}$$

where d is the interionic distance in Å and E_a is expressed in eV.

3. First-principles calculations

3.1. Perfect crystal

The studied alkali halides have the well-known cubic NaCl-like structure (rocksalt), which consists in a face-centered cubic (fcc) array of cations with an interpenetrating fcc anion array (see Fig.3a) [25].

In order to perform the APW + lo calculations, the muffin tin radii (R_{MT}) were chosen in order to allow the relaxation of the structure maintaining non-overlapping atomic spheres (for this purpose we choose R_{MT} values 5% lower than $d/2$). We used R_{MT}-K_{max} = 7 (parameter that controls the size of the basis of eigenfunctions) and 100 k points in the full Brillouin zone, having prior verification of the convergence in the total energy of each system. Once self-consistency of the potential was achieved, the forces on the ions were obtained, and they were moved according to a Newton damped scheme until the forces on the ions were below 0.005 eV/A. This procedure was performed with the WCGGA approximation, which allows the determination of the equilibrium atomic positions (*relaxed structure*), because it provides a functional for the exchange and correlation energy. The relaxed structures obtained by WCGGA were then considered for the calculations with the mBJ method, which does not allow calculating the equilibrium positions.

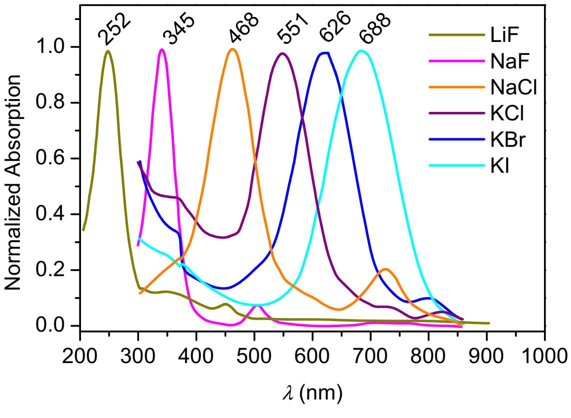

Fig. 1. Normalized absorption spectra for the studied compounds. The peak maxima are indicated in nm.

The density of electronic states (DOS) of NaCl using the WCGGA approximation is shown in Fig. 4a. This system was taken as a representative example of all the studied systems. Fig. 4b and c shows the atom-projected partial DOS for Na and Cl atoms, respectively. According to these figures, the valence band of NaCl is dominated by Cl-3*p* states, with a small contribution of Na orbitals, in agreement with the predominantly ionic nature of this alkali halide. As can be seen there, the conduction band bottom has both Na-*s* and Cl-*s* character, with an admixture of *p* states. The WCGGA calculations predict a band gap of 5.3 eV, which is smaller than the experimental one (8.5(2) eV [26]). Similar results were obtained in the other studied pure alkali halides with WCGGA, *i.e.* the cation and the anion in each alkali halide contribute to the DOS in a similar way to that presented for Na and Cl, respectively. The overall band structures obtained are consistent with previous theoretical results obtained in these systems [27–29]. The Fig. 4d–f shows the total and atom-projected partial DOS for pure NaCl using the mBJ method. This potential diminishes the valence-band width and increases the energy band-gap with respect to those calculated with WCGGA. However, it does not change substantially the internal band structure (see Fig. 4e and f). In this case, using mBJ the calculated band-gap is E_g^{pure} = 8.4 eV, which is in very good agreement with previous calculations [23]. In Table 1 we present the corresponding E_g^{pure} values obtained with the WCGGA approximation and the mBJ method for the seven studied systems. These results demonstrate the general improvement in the prediction of the energy gaps with the mBJ method in comparison to WCGGA, as was shown in previous works for some pure alkali halides [22–24,30]. Therefore, the mBJ calculations, which are barely more expensive than those performed with the WCGGA approximation, are of relevant interest for our study of the defect levels induced by the anion vacancies in alkali halides.

3.2. The F-center

The *F*-center was produced by removing a halogen atom from a supercell of 2 × 2 × 2 times the primitive cell (vacancy atomic total dilution 1:64, see Fig. 3b). This neutral vacancy was treated using a sphere inside which the basis function is atom-like, as done for all the atoms in the structure (i.e., the vacancy is considered as a "ghost atom", without nucleus or electrons). In order to test the chosen APW + lo basis, additional calculations without the atomic sphere at the vacancy site were performed (i.e., treating the vacancy as part of the interstitial region). We found that both methods gave essentially the same results, but the use of the "ghost atom" located at the vacancy site allows the decomposition of the charge density at this site according to the different atomic-like orbitals of the basis. This helps to better understand the role of the vacancy by, for example, performing projections of the DOS at the vacancy site, as already presented in Fig. 4b–c and e–f for the atomic (cation and anion) sites in the perfect crystal.

For all the studied systems, the relaxation process was done using the WCGGA approximation, maintaining the symmetry of the vacancy site (O_h). Since WCGGA leads to reduced energy band-gaps with respect to the experimental values, the position of the defect electronic states introduced by the presence of the impurity is questionable. For this purpose, we used the mBJ

Table 1
Interionic distances *d* (in Å), experimental band-gap energy E_g, and absorption energy E_a for the studied systems. Predictions by WCGGA and mBJ for the energy gap for the pure crystal (E_g^{pure}) and the *F*-center system (E_g^{vac}), and the *s*-*p* transition energy (E_{sp}) are also listed. Energy values are expressed in eV.

System	*d* [25]	Experiment		WCGGA			mBJ		
		E_g^{exp} [26]	E_a	E_g^{pure}	E_g^{vac}	E_{sp}	E_g^{pure}	E_g^{vac}	E_{sp}
KI	3.53	6.0(1)	1.81(2)	4.0	4.3	1.5	6.0	6.1	1.9
KBr	3.30	7.4(2)	1.99(2)	4.4	4.7	1.6	7.3	7.3	2.3
KCl	3.15	8.4(2)	2.26(2)	5.1	5.4	1.8	8.6	8.8	3.0
NaCl	2.81	8.5(2)	2.66(2)	5.3	5.3	2.3	8.4	8.5	3.2
LiCl	2.56	9.4(1)	3.2 [2]	6.1	6.3	2.7	8.7	8.8	3.4
NaF	2.31	11.6(1)	3.61(2)	6.6	6.9	2.9	11.8	12.5	6.0
LiF	2.00	13.6(1)	4.94(2)	9.3	9.4	3.7	13.3	13.7	6.7

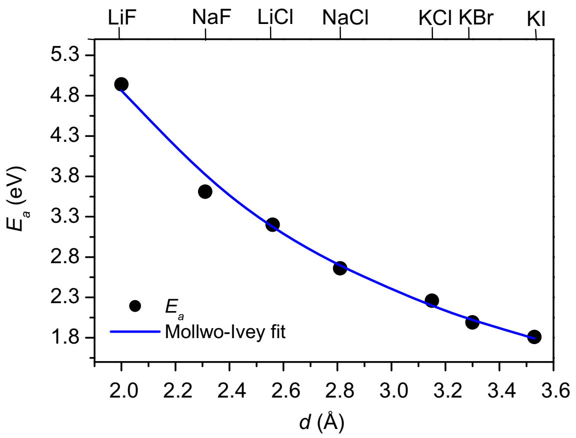

Fig. 2. Experimental absorption energy E_a as a function of the interionic distance *d* (the respective system names are indicated on the top). The blue solid line stands for best least-squares fit of the Mollwo-Ivey relation. (For interpretation of the references to colour in this figure legend, the reader is referred to the web version of this article.)

method, considering the positions of the atoms obtained after the full relaxation process with the WCGGA approximation. As our study is based in ground state calculations, there is no theoretical reason to expect that predictions for the energy transitions between vacancy levels agree exactly with the experimental absorption energies E_a. In this respect, many *ab initio* investigations were performed in order to deal with this issue [4,5,8,31,32] and, recently, different more sophisticated approaches for the treatment of the *F*-center absorption spectra than WCGGA and even mBJ have been proposed and compared in the LiF system [10]. In this work we focus only on the ground-state electronic structure modifications introduced by the anion vacancy over all the proposed alkali halide series.

The removal of the halogen atom in each case leads to structural distortions in the vicinity of the vacancy. According to the WCGGA calculations, the absence of an anion produces a displacement of the six nearest-neighbor cations outward the vacancy of about 1% of the lattice parameter, while the second neighbors (anions) slightly displace inwards the vacancy (changing its positions less than 0.5% of the lattice parameter). This behaviour can be understood in a simple Coulomb interaction scenario if the bound electron generates a weaker attractive force towards the NN cations than that performed by the removed halogen atom. It is worth to notice that, also in related fluoride materials, e.g. CaF_2, BaF_2, and SrF_2, relaxation of the first and second nearest neighbor atoms surrounding the *F*-center are smaller than 1% of the lattice constant parameter [11–13].

Fig. 5a shows the DOS for the NaCl supercell with a chlorine vacancy, obtained with the WCGGA approximation after the relaxation process. We found that this DOS is almost identical to that of the pure crystal (Fig. 4a). Therefore, the structural distortions induced by the vacancy do not produce significant changes in the DOS. For the system with vacancies, the valence band, dominated by the Cl-3*p* states, is separated of the conduction band by an energy gap E_g^{vac} of the same magnitude as that predicted for the pure system (5.3 eV, see Table 1). Fig. 5b and c shows the atom-projected partial DOS for Na and Cl, respectively. In these cases we selected the most distant atoms to the vacancy site (both at about 5 Å from the vacancy and with the major pure crystal-like contributions to the DOS). The vacancy induces the appearance of a partially occupied *s*-type donor level at about 1 eV below the conduction band minimum (see Fig. 5d). In addition, unoccupied

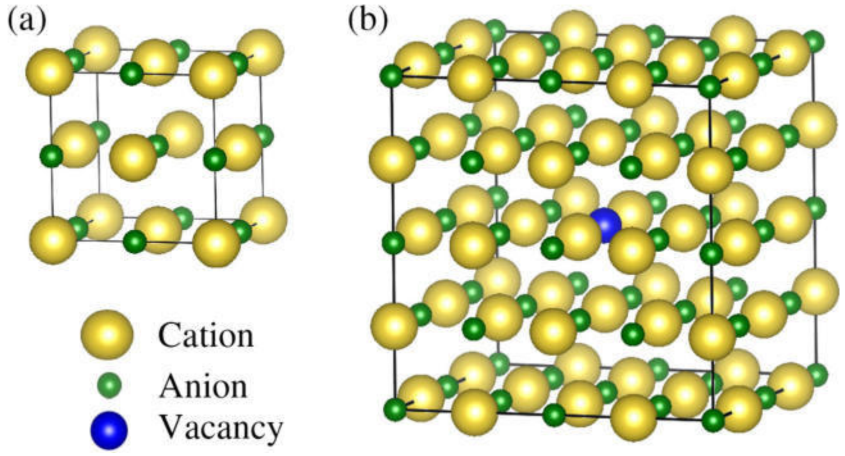

Fig. 3. Cubic NaCl unit cell (a) and 2 × 2 × 2 supercell with an anion vacancy (b).

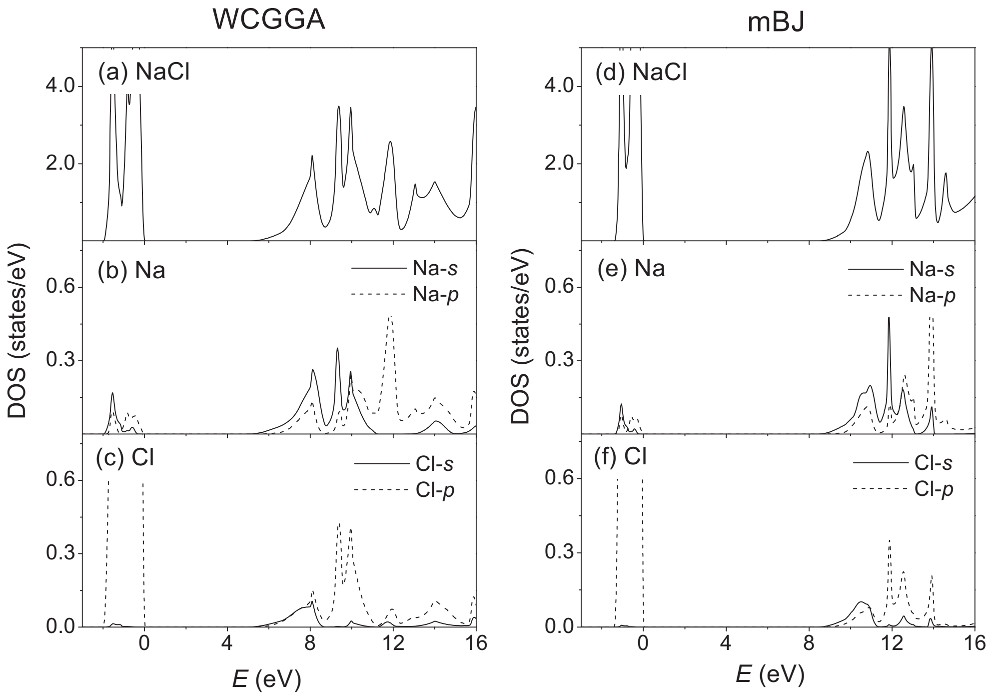

Fig. 4. Calculated total and atom-projected DOSs for pure NaCl predicted by the WCGGA approximation (a–c) and the mBJ method (d–f). For Na and Cl atoms the *s*-(*p*-) type contributions are presented with solid (dashed) lines. Different scales were used on the *y* axes to optimize visibility in all graphs. Energies refer to the highest occupied state.

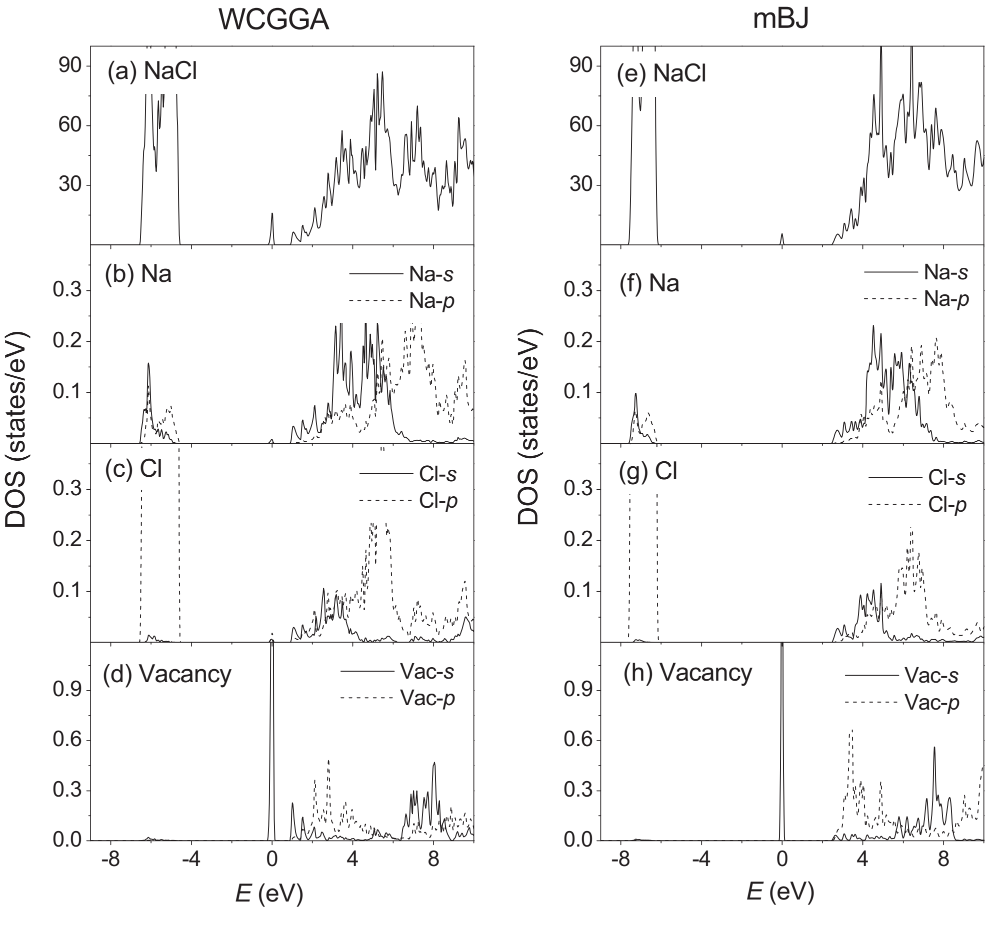

Fig. 5. Calculated total, atom-projected, and vacancy-projected DOSs for the NaCl supercell with an anion vacancy, predicted by the WCGGA approximation (a–d) and the mBJ method (e–h). For Na and Cl atoms, and for the vacancy sphere, the *s*-(*p*-) type contributions are presented with solid (dashed) lines. Different scales were used on the *y*-axes to optimize visibility in all graphs. Energies refer to the highest occupied state.

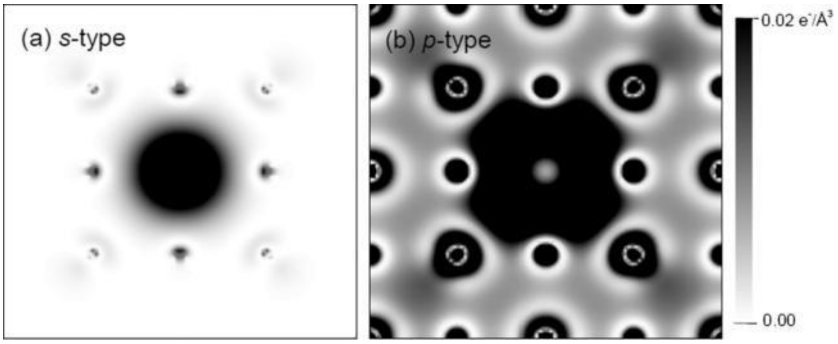

Fig. 6. Electron density projections for the vacancy electronic states in NaCl in the plane [1 0 0] and for states with energies in the range of the (filled) *s*-type state (a) and the (empty) *p*-type state (b) (see text). The vacancy site is at the center of each picture.

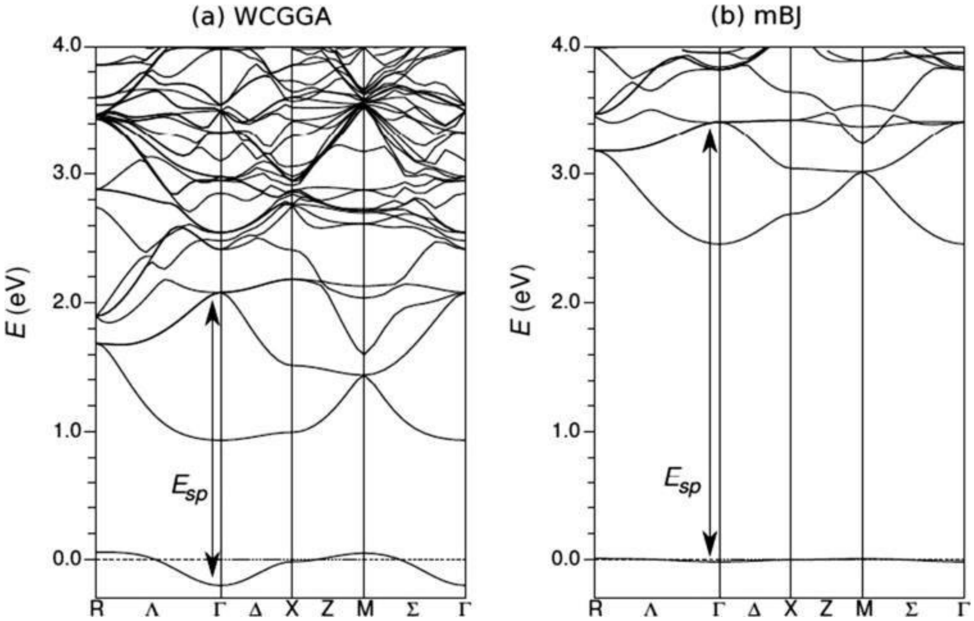

Fig. 7. Electronic band structure near the conduction band bottom for the NaCl supercell with an anion vacancy, calculated with the WCGGA approximation (a) and the mBJ method (b). The E_{sp} transition is at Γ point. Energies refer to the highest occupied state.

p-type vacancy states in the conduction band are found. The DOS obtained with the mBJ method for this system with vacancy presents the same features than those sketched in Fig. 5a-d, with differences arising from the prediction of a larger E_g value (E_g^{vac}=8.5 eV). It can be seen that this method increases the distance of the *s*-type vacancy state to the conduction band. Also, it is observed that the *p*-type vacancy states tend to localize on the conduction band bottom (Fig. 5h).

The spatial electron density projections corresponding to the states with energies in the range of the (filled) *s*-type and (empty) *p*-type vacancy levels are plotted in Fig. 6. At the center of each of these pictures is the vacancy site. The four nearest-neighbors are Na atoms (at ±*d* along the vertical and horizontal direction), and the next neighbors are Cl atoms (at $\sqrt{2}d$ from the vacancy site, along the diagonal). In Fig. 6a there are projected the 0.40 electrons that occupy the *s*-type donor level. This plot shows that the donor level found in the DOS (Fig. 5d) has a correspondence with a highly localized electron density distribution inside the vacancy site (i.e. a bounded electron) for the ground state. This good description to within two lattice parameter demonstrates that the proposed supercell approach is good enough to treat the *F*-center. In the same way, the first 0.4 electrons that occupy the energy range of the *p*-type states in the conduction band bottom are projected in Fig. 6b. In this case, it can be seen that those electrons are more delocalized.

The *s*-*p* energy difference (E_{sp}, for which we consider the first *p*-type peak inside the conduction band, see Fig. 5d and h) is 2.3 eV with the WCGGA approximation, and 3.2 eV with the mBJ method. In Fig. 7 we present the corresponding electronic band structures for NaCl, in an energy region that includes the vacancy donor level and the first states in the conduction band bottom. The E_{sp} energy corresponds to the $a_{1g} \rightarrow t_{1u}$ direct transition at the Γ point, and passes over the conduction band minimum, which does not have *p*-character (as shown in Fig. 5d and h). The calculated values of E_{sp} are in good agreement with the experimental absorption energy E_a (2.66(2) eV, see Table 1).

At this point it is important to mention that if we consider an indirect transition such as $\Gamma \rightarrow X$ or $\Gamma \rightarrow M$, for which the final states have a weak *p*-type vacancy character, the corresponding transition energies are lower than E_{sp} (see Fig. 7). If we consider the WCGGA approximation, the mentioned indirect transitions start at 1.6 eV. Otherwise, if we consider the mBJ calculations, for the $\Gamma \rightarrow X$ transition we obtain 2.7 eV, which is 0.5 eV lower than the E_{sp} value. Because the E_{sp} prediction with the mBJ method over-

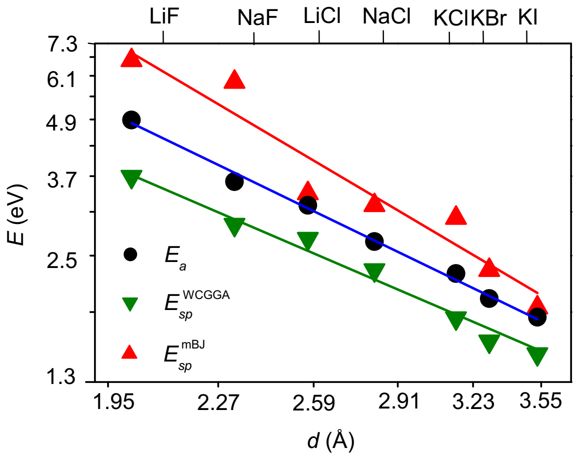

Fig. 8. Experimental absorption energy E_a and calculated E_{sp} energies as a function of the interionic distance d (the respective system names are indicated on the top). Solid lines are best least-squares fits of the Mollwo-Ivey relation for each data set (see text).

estimates E_a, by considering the indirect transitions predicted by this potential we found a better agreement with the measurements. This fact shows, as mentioned above, that the band gap problem strongly affects the correct description of the defect levels (as shown in Fig. 5). In this respect, other authors obtained similar predictions when used DFT methods that subestimate E_g [4,7]. Therefore, the use of a semilocal exchange and correlation potential as implemented in the mBJ method emerges as a more suitable procedure than the WCGGA for the description of these systems with vacancies. In this work we demonstrated that the mBJ method gives an accurate prediction of the E_g value, and simultaneously rearranges the relative position of the *s*- and *p*-type vacancy states, giving E_{sp} values in a better agreement with the experimental energy E_a than those calculated with WCGGA.

In Table 1 we list the E_g^{vac} and E_{sp} energies for all the studied systems with an anion vacancy, obtained by WCGGA and mBJ. Both energies increase with decreasing the interionic distance d. As can be seen in Table 1, in general, the energy gaps of the system with vacancy (E_g^{vac}) are slightly larger than those of the pure compound (E_g^{pure}), being the differences between them below 8%. Concerning E_{sp}, for KI the difference between the predictions obtained by both methods is minimum (0.4 eV), and for NaF and LiF (which have the minimum distances d among the studied alkali halides) this difference reaches its maximum (3.1 and 3.0 eV, respectively). Depending on the studied compound and the method of calculation, the predicted E_{sp} energy represents 30–50% of E_g^{vac}, and by mBJ the E_{sp}/E_g^{vac} ratio decreases monotonously with d. Additionally, it can be noted that the distance from the a_{1g} level to the conduction band minimum (at Γ point, see Fig. 7) also decreases monotonously with d. If we compare our theoretical predictions with the experimental measurements, the E_{sp} energies obtained by WCGGA subestimate the absorption energy E_a (E_{sp} values are 15–25% lower than E_a), while by mBJ the E_{sp} energies overestimates E_a (E_{sp} values are 5–66% higher than E_a). However, as we concluded for NaCl, considering the possible indirect transitions, the latter method is more suitable for the comparison with experimental results. Fig. 8 shows the results for the experimental E_a and the theoretical E_{sp} energies as a function of d, and the corresponding power-law relation fits. We obtain for the WCGGA calculations ${E_{sp}}^{\mathrm{WCGGA}}(d) = 12(1)\ d^{-1.6(1)}$, and for the mBJ method ${E_{sp}}^{\mathrm{mBJ}}(d) = 31(8)\ d^{-2.2(3)}$, where d is expressed in Å and E_{sp} in eV. These relations agree with the experimental trend obtained for $E_a(d)$ and delimit the Mollwo-Ivey relation of Eq. (1). For the mBJ method, the predicted ${E_{sp}}^{\mathrm{mBJ}}(d)$ power-law relation is in perfect agreement with the simpler models based in a Schrödinger-like problem of an electron trapped in a potential well (according to this treatment E_a has d^{-2} dependence), which were often proposed in the very beginning of the study of these systems [2,33]. However, the success of this non-*ab initio* models depends on arbitrary values for the potential width and depth.

4. Summary and conclusions

We revisited experimentally the characterization of the absorption energies E_a in *F*-centers in alkali halides, and we analysed by first-principles the structural and electronic properties of the anion vacancy. Using the proposed supercell approach with an atomic sphere description of the vacancy site ("ghost atom" approach), we demonstrated that the bounded electron is localized to within two lattice parameter. We observed that the structural distortions induced by the vacancy do not affect significantly the DOS of the studied compounds, except for the introduction of the donor vacancy states. For all the studied systems with vacancies, an *s*-type defect level is found isolated, near the conduction band minimum, together with the *p*-type states localized at the bottom of the conduction band. We showed that the mBJ method performs accurate predictions for the energy band gap E_g and gives values for the *s*-*p* transition energies in better agreement with the experimental E_a than those obtained with WCGGA.

Acknowledgements

This work was partially supported by Consejo Nacional de Investigaciones Científicas y Técnicas (CONICET) under Grant No. PIP0803, Argentina. This research made use of the computational facilities of the Physics of Impurities in Condensed Matter (PhI) group and the HPPC BOSE Cluster at IFLP and Departamento de Física (UNLP). The Chemistry Department (Facultad de Ciencias Exactas, UNLP) is kindly acknowledged for facilitating the UV/VIS experimental facilities. DR and MR (JH) are (is) members (fellow) of CONICET, Argentina.

References

[1] C. Kittel, Introduction to Solid State Physics, fifth ed., Wiley, 1976.
[2] J.J. Markham, in: F. Seitz, D. Turnbull (Eds.), F-centers in alkali halides, Academic Press, 1966.
[3] M.S. Malghani, D.Y. Smith, Phys. Rev. Lett. 69 (1992) 184–187.
[4] M.R. Pederson, B.M. Klein, Phys. Rev. B 37 (1988) 10319–10331.
[5] M.P. Surh, H. Chacham, S.G. Louie, Phys. Rev. B 51 (1995) 7440–7464.
[6] R.F.W. Bader, J.A. Platts, J. Chem. Phys. 107 (1997) 8545–8553.
[7] C.M. Fang, R.A. De Groot, J. Phys.: Condens. Matter 20 (2008) 075219.
[8] W. Chen, C. Tegenkamp, H. Pfnür, T. Bredow, Phys. Rev. B 82 (2010) 104106.
[9] C. Ma, T. Liu, Q. Chang, Comp. Theor. Chem. 1080 (2016) 79–83.
[10] F. Karsai, P. Tiwald, R. Laskowski, F. Tran, D. Koller, S. Gräfe, J. Burgdöfer, L. Wirtz, P. Blaha, Phys. Rev. B 89 (2014) 125429.
[11] H. Shi, L. Chang, R. Jia, R.I. Eglitis, J. Phys. Chem. C 116 (2012) 4832–4839.
[12] H. Shi, R. Jia, R.I. Eglitis, Solid State Ion. 187 (2011) 1–7.
[13] H. Shi, L. Chang, R. Jia, R.I. Eglitis, Comput. Mater. Sci. 79 (2013) 527–533.
[14] R.I. Eglitis, N.E. Christensen, E.A. Kotomin, A.V. Postnikov, G. Borstel, Phys. Rev. B 56 (1997) 8599.
[15] D. Ricci, G. Bano, G. Pacchioni, F. Illas, Phys. Rev. B 68 (2003) 224105.
[16] E. Cho, S. Han, H. Ahn, K. Lee, S.Keun Kim, C.Seong Hwang, Phys. Rev. B 73 (2006) 193202.
[17] A.F. Fix, F.U. Abuova, R.I. Eglitis, E.A. Kotomin, A.T. Akilbekov, Phys. Scr. 86 (2012) 035304.
[18] M. Gerosa, C.E. Bottani, L. Caramella, G. Onida, C. Di Valentin, G. Pacchioni, J. Chem. Phys. 143 (2015) 134702.
[19] P. Blaha, K. Schwarz, G.K.H. Madsen, D. Kvasnicka, J. Luitz, WIEN2k, An Augmented Plane Wave + Local Orbitals Program for Calculating Crystal Properties, Karlheinz Schwarz, Techn. Universität Wien, Austria, 2001.
[20] Z. Wu, R.E. Cohen, Phys. Rev. B 73 (2006) 235116.
[21] I.N. Yakovkin, P.A. Dowben, Surf. Rev. Lett. 14 (2007) 481–487.
[22] F. Tran, P. Blaha, Phys. Rev. Lett. 102 (2009) 226401.
[23] D. Koller, F. Tran, P. Blaha, Phys. Rev. B 85 (2012) 155109.
[24] J.A. Camargo-Martínez, R. Baquero, Phys. Rev. B 86 (2012) 195106.

[25] R.W.G. Wyckoff, Crystal Structures, vol. 1, 2nd ed., Wiley, 1965.
[26] R.T. Poole, J.G. Jenkin, J. Liesegang, R.C.G. Leckey, Phys. Rev. B 11 (1975) 5179–5189.
[27] W.Y. Ching, F. Gan, M.Z. Huang, Phys. Rev. B 52 (1995) 1596–1611.
[28] P.K. de Boer, R.A. de Groot, Am. J. Phys. 67 (1999) 443–445.
[29] P.K. de Boer, R.A. de Groot, Phys. Lett. A 256 (1999) 227–229.
[30] H. Jiang, J. Chem. Phys. 138 (2013) 134115.
[31] J. Carrasco, C. Sousa, F. Illas, P.V. Sushko, A.L. Shluger, J. Chem. Phys. 125 (2006) 074710.
[32] P. Rinke, A. Schleife, E. Kioupakis, A. Janotti, C. Rödl, F. Bechstedt, M. Scheffler, C.G. Van de Walle, Phys. Rev. Lett. 108 (2012) 126404.
[33] J.F. Reichert, Am. J. Phys. 51 (1983) 431–433.

INTERNATIONAL JOURNAL OF HYDROGEN ENERGY XXX (2013) 1–5

Available online at www.sciencedirect.com

ScienceDirect

journal homepage: www.elsevier.com/locate/he

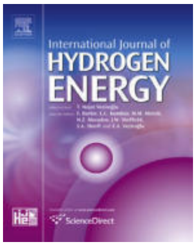

Mechanical milled doped Zn-based semiconductors powders for photovoltaic devices

J.I. Laborde[a], J. Hoya[a], M.D. Reyes Tolosa[b], M.A. Hernandez-Fenollosa[b], L.C. Damonte[a,c,*]

[a] Departamento de Física, Facultad de Ciencias Exactas, Universidad Nacional de La Plata (UNLP), CC 67, 1900 La Plata, Argentina
[b] Instituto de Tecnología de Materiales, Universitat Politècnica de València, 46022 Camino de Vera s/n, Valencia, Spain
[c] Instituto de Física La Plata (IFLP, CONICET), La Plata, Argentina

ARTICLE INFO

Article history:
Received 21 October 2013
Accepted 5 December 2013
Available online xxx

Keywords:
Nanocrystalline semiconductors
Mechanical milling
Photovoltaic cells

ABSTRACT

Structural characterization of nanocrystalline Al-doped ZnTe semiconductors, obtained by mechanical milling from ZnTe and Al_2O_3 powders, is presented. The samples were analyzed by X-ray diffraction (XRD), scanning electron microscopy (SEM), X-ray absorption full spectroscopy (XAFS) and positron annihilation lifetime (PALS) measurements. The results suggested that Al atoms are substitutional incorporated into the ZnTe cubic structure.

1. Introduction

Among II–VI semiconductors zinc telluride (ZnTe) is very attractive for optoelectronic device applications in the green spectral range, due to its direct wide band gap (~2.26 eV) [1–3]. It usually has a cubic crystal structure; it is a material of high absorption coefficient and shows p-type characteristics. Since zinc telluride can be easily doped and being a low cost semiconductor material, it can be used as different constituent for solar cells, for example, as a back-surface field layer and p-type semiconductor material for a CdTe/ZnTe structure [3–5] or as the inorganic element in hybrid solar cells. ZnTe alloys have been obtained with different morphologies and using a variety of methods such as electrodeposition [6], pulsed laser deposition (PLD) [7], thermal evaporation [8,9], molecular beam epitaxy (MBE), magnetron sputtering [10] and mechanical alloying techniques [11,12].

Mechanical alloying (MA) is a room temperature solid-state route able of synthesizing a variety of equilibrium and non-equilibrium alloys, including nanocrystalline phases and amorphous compounds [13,14]. This technique in addition to its versatility has many advantages, like low cost, easy control of composition and large scale production.

It is known that solar cells efficiency may be improved increasing charge carriers densities and interfacial processes. New kind of materials, different assemblies, etc has been studied during the last decades. In particular, the development of nanomaterials production has opened a great amount

---

[*] *Corresponding author*. Instituto de Física La Plata (IFLP, CONICET), 1900 La Plata, Argentina.
E-mail addresses: mareto@upvnet.upv.es (M.D. Reyes Tolosa), mhernan@upvnet.upv.es (M.A. Hernandez-Fenollosa), damonte@fisica.unlp.edu.ar, lcdamonte@gmail.com (L.C. Damonte).

0360-3199/$ – see front matter Copyright © 2013, Hydrogen Energy Publications, LLC. Published by Elsevier Ltd. All rights reserved.
http://dx.doi.org/10.1016/j.ijhydene.2013.12.051

Please cite this article in press as: Laborde JI, et al., Mechanical milled doped Zn-based semiconductors powders for photovoltaic devices, International Journal of Hydrogen Energy (2013), http://dx.doi.org/10.1016/j.ijhydene.2013.12.051

of research in this area. In this sense, our goal is investigate nanopowders and nanocolumns, prepared by low cost methods [15,16] and its doping with donor elements. In previous works we have successfully obtained ZnO nanopowders and nanocolumns doped with Al and In and analyzed their structural and optical properties [16,17].

Recently, other II–VI semiconductor as ZnTe and ZnSe were subjected to mechanical work and their structural characteristic were studied by means of X-ray diffraction and positron annihilation measurements.

In this work, we concentrate in the Al doping of ZnTe by mechanical milling and its structural characterization. Nanosized doped powders were analyzed by X-ray diffraction, X-ray Absorption Full Spectroscopy (XAFS), scanning electron microscopy (SEM) and positron annihilation lifetime (PALS) measurements. The results, compared with undoped powders, will allow us to improve the performance of hybrid organic/inorganic solar cells.

2. Experimental procedure

Stoichiometric quantities were weighed to obtain mixtures of ZnTe (99.99% from Aldrich Chemistry) with 5 at% Al_2O_3 (99.9%), powders provided by Alfa Aesar Johnson Matthey Co. The powders were milled in a steel cylinder (8 cm^3) with one steel ball (diameter 12 mm) in air atmosphere being the ball mass to powder mass ratio of 10/1. The mechanical milling was performed in a Retsch MM2 horizontal vibratory mill at a frequency of 30 Hz during different milling times (1, 5 and 10 h).

Starting and milled powders were characterized by X-Ray diffraction (XRD) performed with a Philips PW1710 Diffractometer with CuKα radiation in the National Diffraction Laboratory (LANADI-UNLP).

Powder microstructure was also investigated by scanning electron microscopy (SEM) with a JSM–6300 (JEOL Scanning Microscopy) operating at 10 kV in the UPV (Valencia – Spain).

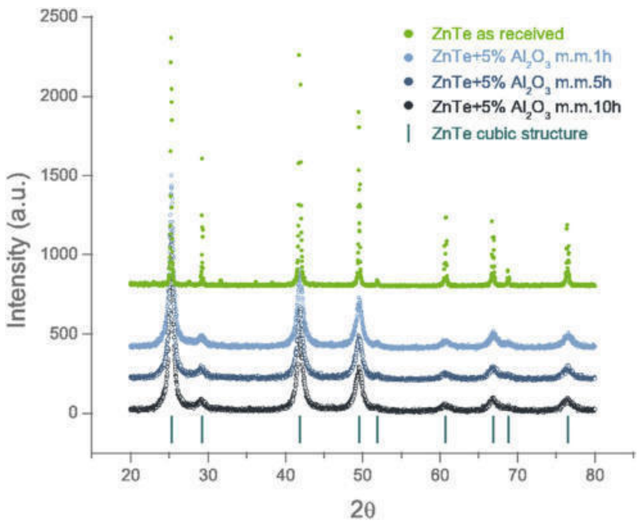

Fig. 1 – X-ray diffractograms for pure and doped ZnTe, at different milling times.

X-ray Absorption Full Spectroscopy (XAFS) measurements were taken at room temperature in transmission mode at the Zn K-edge, using a Si(111) monochromator at the XAFS1 beam line of LNLS (Campinas, Brazil).

Milled powders were then compacted under uniaxial pressure of 150 MPa into disk-shaped pellets (diameter 8 mm).

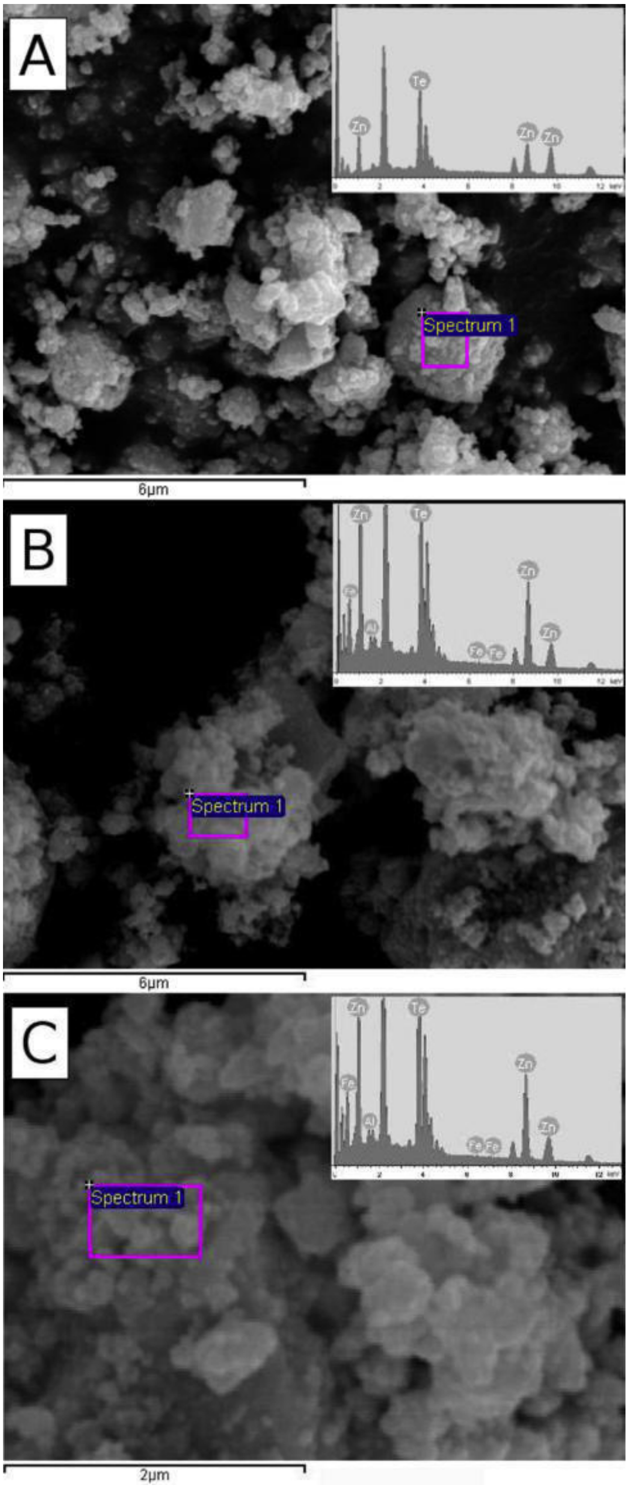

Fig. 2 – SEM micrographs for: A) pure ZnTe after 10 h of milling; B) and C) Al-doped ZnTe after 1 and 10 h of milling. Insent show EDS analysis at the signed region.

Please cite this article in press as: Laborde JI, et al., Mechanical milled doped Zn-based semiconductors powders for photovoltaic devices, International Journal of Hydrogen Energy (2013), http://dx.doi.org/10.1016/j.ijhydene.2013.12.051

Positron Annihilation Lifetime measurements (PALS) were done in a conventional fast–fast coincidence system with two scintillator detectors (one BaF_2 and one plastic BURLE) provided a time resolution (FWHM) of 260 ps. A $^{22}NaCl$ (10 μCi) radioactive source deposited onto a kapton foil (1.42 g/cm^3) and sandwiched between two identical samples was used. The source contribution and the response function were evaluated from a Hf metal reference sample using the RESOLUTION code [18]. Positron lifetime spectra of 3×10^6 counts each were recorded at room temperature and analyzed with the POSITRONFIT program [18].

3. Results and discussion

The XRD patterns for the ZnTe powders, as received and milled 1, 5 and 10 h with 5 at% Al_2O_3, are shown in Fig. 1. For all of them, the diffractograms display the reflection lines of cubic (F43m) ZnTe, with a peak broadening, consequence of grain size reduction [19]. For doped samples no additional peaks are observed, even for those samples after low milling times where a low contribution from Al_2O_3 is expected.

Fig. 2 shows SEM micrographs for pure and Al-doped ZnTe after milling. The inset displays EDS analysis result at the indicated site. As milling proceeds, grain size diminution and agglomeration are observed. In Al-doped samples, the presence of Fe atoms, evidenced from EDS analysis, indicate iron contamination from milling tools. The Fe atomic % increases with milling time from 0.19 to 0.59, while for pure ZnTe no contamination is observed even after 10 h of milling. This low content of Fe was not reported in the X-ray analysis.

In order to get information on doping atom incorporation into the host semiconductor some XAFS analysis were done. Fig. 3 shows the XAFS function χ(R) for Al-doped ZnTe as function of milling time. For comparison undoped ZnTe is also shown. The results were analyzed using the IFFEFIT software, with the Athena implementation. In a very preliminary way, we conclude that the distance from Zn to nearest neighbours do not change, neither with milling time nor with the addition of dopants. There is a diminution in the principal peak amplitude in all cases with respect the starting material. Also, both, milling and doping processes have a little effect at low values of R to the left of the main peak.

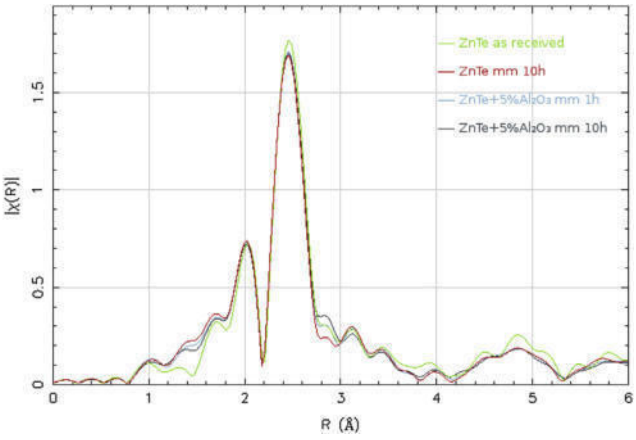

Fig. 3 – XAFS function for pure and doped ZnTe as milling time increases.

Fitting procedure was carried out using the FEFF7 phase and amplitudes. The ATOMS code was used as a tool to generate the input files for FEFF7 based on the ZnTe crystallography data. The Fourier Transformed (FT) EXAFS data of ZnTe starting sample is shown in Fig. 4. If TeO_2 is include not significant improvement is observed. Instead, for milled pure and doped ZnTe the inclusion of zinc and telluride oxide, improve the fits at low values of R. We take into account only the first coordination sphere of both oxides that corresponds to Zn–O and Te–O distances. Although this incorporation, they have relatively low amplitudes. Moreover, we try the inclusion of Al_2O_3 or Al metal in order to analyze the incorporation of the dopant atom into the ZnTe structure but the final fit was not better. The results are shown in Fig. 5.

The lifetime spectra for all samples consist in various exponential decays

$$n(t) = \sum_i I_i \exp(-t/\tau_i)$$

being the relative intensities I_i, normalized, $S_i = 1$. After background subtraction, and convolution with the resolution function, the parameters that characterized each positron state, λ_i annihilation rate ($\lambda_i = 1/\sigma_i$) and its intensity I_i, are obtained by means of POSITRONFIT program [18]. The PALS spectra were decomposed into two exponential decays, assuming a source correction with two components, one of 386 ps of 15% intensity assigned to kapton foil and a second one of around 1 ns with less than 1% intensity due to annihilation in the surroundings of the source. The presence of two lifetime components is an usual feature for II–VI semiconductors compounds, since intrinsic and extrinsic defects introduced during crystal growth and doping are unavoidable [20]. Also mechanical milling introduces a certain amount of defects such as vacancies, interstitials, etc [13]. All these point defects constitute positron trapping centers leading to similar positron lifetime components unable to be separate. So we have evaluated the average positron lifetime defined by

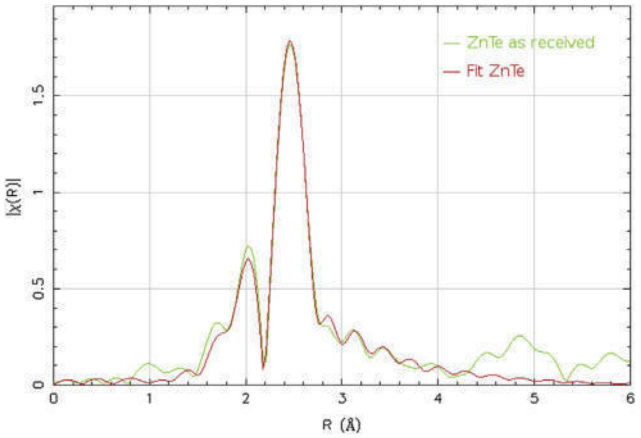

Fig. 4 – χ(R) for pure ZnTe, red line represent the result of the fit. (For interpretation of the references to color in this figure legend, the reader is referred to the web version of this article.)

Please cite this article in press as: Laborde JI, et al., Mechanical milled doped Zn-based semiconductors powders for photovoltaic devices, International Journal of Hydrogen Energy (2013), http://dx.doi.org/10.1016/j.ijhydene.2013.12.051

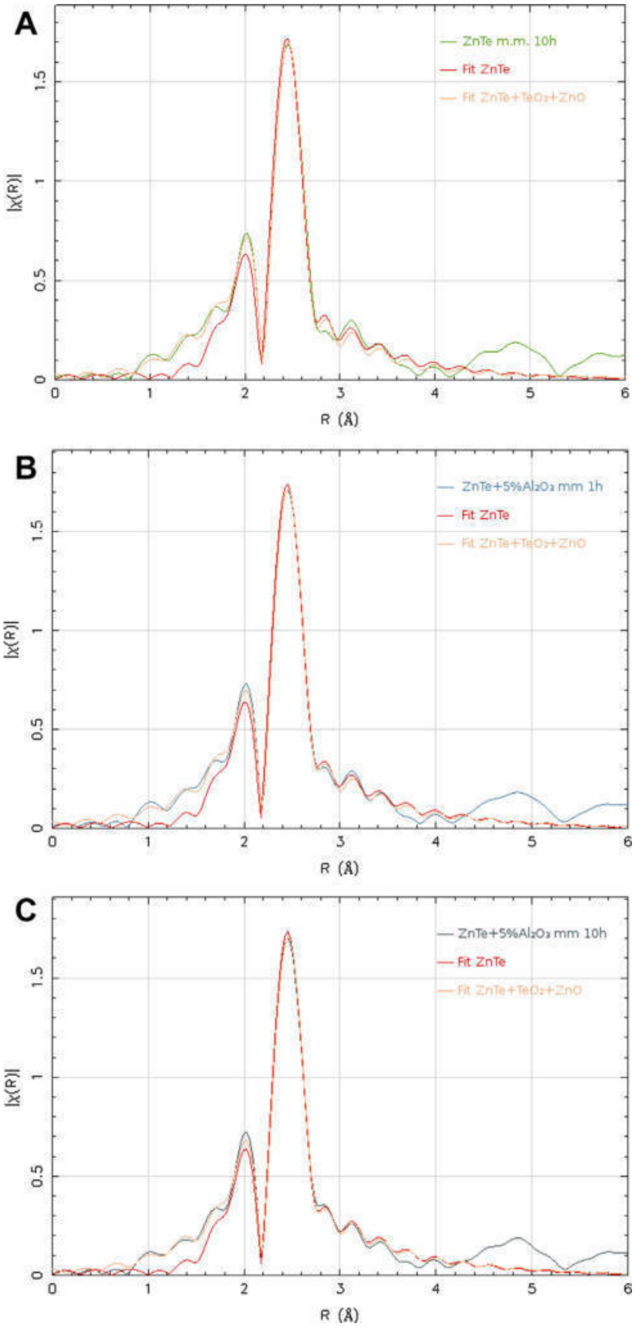

Fig. 5 – χ(R) data together with fitting results: A) pure ZnTe, B) Al-doped ZnTe after 1 h of milling, C) Al-doped ZnTe after 1° h of milling. Orange lines represent the result of the fit including the oxides. (For interpretation of the references to colour in this figure legend, the reader is referred to the web verson of this article.)

$$\tau_{ave} = \sum_i I_i \tau_i$$

a useful parameter almost independent of data treatment. From this statistical parameter, one can extract information about the evolution of positron traps.

The resulting values for pure and doped zinc telluride are summarized in Table 1.

Table 1 – Average positron lifetime for pure and Al-doped ZnTe.

Sample	Milling time (h)	τ_{ave}(ps)
ZnTe	0	321
	10	342
Al–ZnTe	0	351
	5	353
	10	357

It can be seen that the values for Al-doped ZnTe are similar to the pure and milled compound. As was already conclude for doped ZnO [16], this fact can be interpreted as an incorporation of doping atom into the semiconductor structure since no other lifetime contribution is observed.

4. Conclusions

It is proved that mechanical milling is a simple, cheap and effective method to obtain nanocrystalline aluminum doped zinc telluride powders from ZnTe and Al_2O_3 mixtures. From X-ray diffraction and SEM images the nanocrystalline nature of the powders is confirm. Also, no trace is observed of other compounds than ZnTe. XAFS measurements gave information of a kind of surface oxidation since the results admit a small contribution of ZnO and TeO_2. In addition, since no aluminum compound can be included in the analysis they also give evidence of aluminum incorporation into the ZnTe crystalline structure. Moreover, positron annihilation lifetime spectroscopy became an effective tool to sense dopant incorporation into ZnTe power through the average lifetime evolution with milling time. However, a slight iron contamination from milling tools is observed from EDS analysis for the doped samples.

Optical characterization is now in course in order to give support to dopant incorporation into the semiconductor structure and its effect on the specific properties towards their photovoltaic applications.

Acknowledgments

This work was supported by the CONICET (PIP 112-200802-00128) from Argentina. Authors also acknowledge Dr. Marcos Meyer for his collaboration.

REFERENCES

[1] Kvit A, Oktyabrsky S. Defects in CdTe and related compounds encyclopedia of materials: science and technology. 2nd ed.; 2001. pp. 1985–9.
[2] Hakan Gürel H, Ünlü Hilmi. Density functional and tight binding theories of electronic properties of II–VI heterostructures. Mat Sci Semicond Process 2013;16:1619–28.
[3] Gilic M, Romcevic N, Romcevic M, Stojanovic D, Kostic R, Trajic J, et al. Optical properties of CdTe/ZnTe self-assembled quantum dots: Raman and photoluminescence spectroscopy. J Alloys Compd 2013;579:330–5.

Please cite this article in press as: Laborde JI, et al., Mechanical milled doped Zn-based semiconductors powders for photovoltaic devices, International Journal of Hydrogen Energy (2013), http://dx.doi.org/10.1016/j.ijhydene.2013.12.051

[4] Feng X, Singh K, .Bhavanam S, Palekis V, Morel D-L, Ferekides C. Preparation and characterization of ZnTe as an interlayer for CdS/CdTe substrate thin film solar cells on flexible substrates. Thin Solid Films 2013;535:202–5.

[5] Kozlovsky VI, Krysa AB, V Korostelin Yu, .G Sadofyev Yu. MBE growth and characterization of ZnTe epilayers and ZnCdTe/ZnTe structures on GaAs(1 0 0) and ZnTe(1 0 0) substrates. J Crystal Growth 2000;214–215:35–9.

[6] Jiang Y, Kou H, Li J, Yu S, Du Y, Ye W, et al. Synthesis of ZnTe dendrites on multi-walled carbon nanotubes/polyimide nanocomposite membrane by electrochemical atomic layer deposition and photoelectrical property research. J Solid State Chem 2012;194:336–42.

[7] Ghosh B, Ghosh D, Hussain S, Bhar R, Pal AK. Growth of ZnTe films by pulsed laser deposition technique. J Alloys Compd 2012;541:104–10.

[8] Ko H, Park S, An S, Lee C. Intense near-infrared emission from undoped ZnTe nanostructures synthesized by thermal evaporation. J Alloys Compd 2013;580-15:316–20.

[9] Güllü HH, Bayraklı Ö, Candan İ, Coşkun E, Parlak M. Structural and optical properties of Zn–In–Te thin films deposited by thermal evaporation technique. J Alloys Compd 2013;566:83–9.

[10] Zhang Z, Li J, Zhang H, Pan X, Xie E. Thickness-dependent field emission from ZnTe films prepared by magnetron sputtering. J Alloys Compd 2013;549:88–91.

[11] Hoya J, Laborde JI, Damonte LC. Structural characterization of mechanical milled ZnSe and ZnTe powders for photovoltaic devices. Int J Hydrogen Energy 2012;37:14769–72.

[12] Patra S, Pradhan SK. Quickest single-step one pot mechanosynthesis and characterization of ZnTe quantum dots. J Alloys Compd 2011;509:5567–70.

[13] Suryanarayana C. Mechanical alloying and milling. Progr Mater Sci 2001;46(1):184.

[14] Damonte LC, Mendoza-Zélis LA, Deledda S, Eckert J. Effect of preparation conditions on the short-range order in Zr-based bulk glass-forming alloys. Mat Sc and Eng 2003;A343:194–8.

[15] Damonte LC, Donderis V, Ferrari S, Meyer M, Orozco J, Hernández Fenollosa MA. ZnO-based nanocrystalline powders with applications in hybrid photovoltaic cells. Int Journal of Hydrogen Energy 2010;35:5834–7.

[16] Reyes Tolosa MD, Orozco-Messana J, Damonte LC, Hernandez-Fenollosa MA. ZnO nanoestructured layers processing with morphology control by pulsed electrodeposition. J Electrochem Soc 2011;158:D452–5.

[17] Damonte LC, Donderis V, Hernández Fenollosa MA. Trivalent dopants on ZnO semiconductor obtained by mechanical milling. J Alloys Compd 2009;483(1–2):442–84.

[18] Kirkegaard P, Pedersen NJ, Eldrup M. PATFIT-88 Riso-M-2740; 1989. Risø.

[19] Damonte LC, Mendoza Zélis LA, Marí Soucase B, Hernández Fenollosa MA. Nanoparticles of ZnO obtained by mechanical milling. Powder Technol 2004;148:1519.

[20] Krause-Rehberg R, Leipner HS, Abgarjan T, Polity A. Review of defect investigations by means of positron annihilation in II-VI compound semiconductors. Appl Phys A 1998;66:599–614.

Please cite this article in press as: Laborde JI, et al., Mechanical milled doped Zn-based semiconductors powders for photovoltaic devices, International Journal of Hydrogen Energy (2013), http://dx.doi.org/10.1016/j.ijhydene.2013.12.051

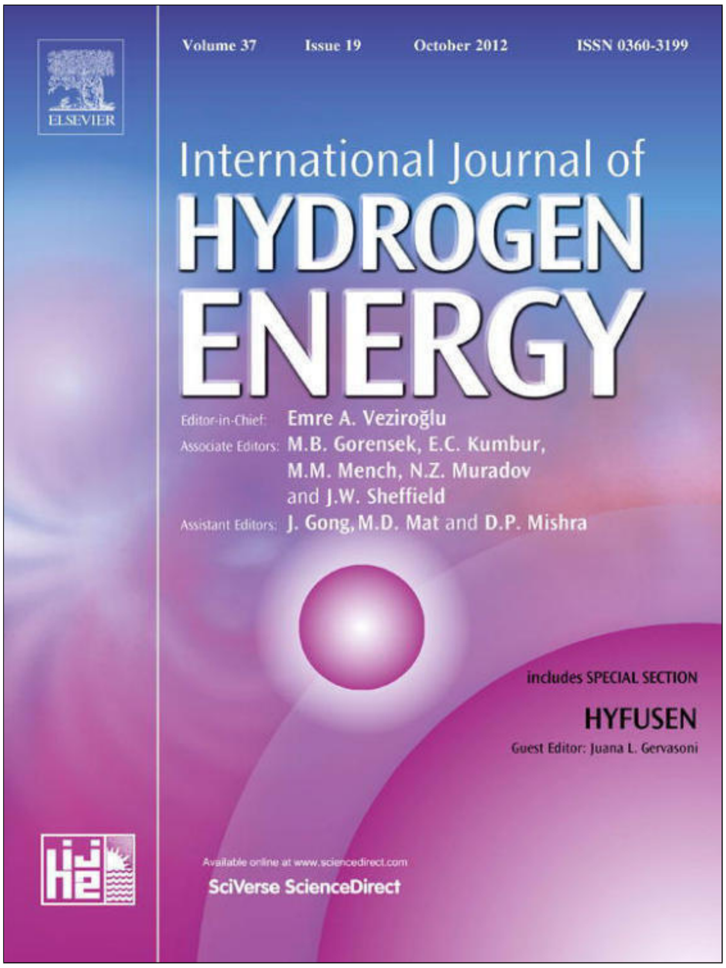
Volume 37
Issue 19
October 2012
ISSN 0360-3199
ELSEVIER
International Journal of
HYDROGEN
ENERGY
Editor-in-Chief: Emre A. Veziroğlu
Associate Editors: M.B. Gorensek, E.C. Kumbur, M.M. Mench, N.Z. Muradov and J.W. Sheffield
Assistant Editors: J. Gong, M.D. Mat and D.P. Mishra
includes SPECIAL SECTION
HYFUSEN
Guest Editor: Juana L. Gervasoni
Available online at www.sciencedirect.com
SciVerse ScienceDirect

INTERNATIONAL JOURNAL OF HYDROGEN ENERGY 37 (2012) 14769–14772

Available online at www.sciencedirect.com

SciVerse ScienceDirect

journal homepage: www.elsevier.com/locate/he

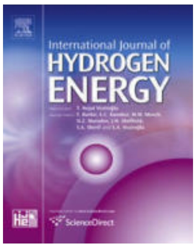

Structural characterization of mechanical milled ZnSe and ZnTe powders for photovoltaic devices

J. Hoya [a], J.I. Laborde [a], L.C. Damonte [a,b,*]

[a] Departamento de Física Prof. Emil H. Bose, Facultad de Ciencias Exactas, Universidad Nacional de La Plata, CC 67, 1900 La Plata, Buenos Aires, Argentina
[b] Instituto de Física La Plata (IFLP, CONICET), La Plata, Buenos Aires, Argentina

ARTICLE INFO

Article history:
Received 12 September 2011
Accepted 12 December 2011
Available online 4 January 2012

Keywords:
Nanocrystalline semiconductors
Positron annihilation
Mechanical milling

ABSTRACT

II–VI semiconductors are of interest due to their potential application as photovoltaic devices like hybrid solar cells. The efficiency of these devices may be improved mainly increasing charge carriers densities and interfacial processes. In order to reach this last purpose nanocrystalline materials are the best option as solar cells constituents. In this work we present a structural characterization of nanocrystalline ZnSe and ZnTe semiconductors obtained by mechanical milling. The samples were analyzed by X-ray diffraction (XRD), scanning electron microscopy (SEM) and positron annihilation lifetime (PALS) measurements. PALS results were compared with ab-initio simulations using the MIKA program. The two-component density functional theory framework (TC-DFT) with the generalized gradient approximation (GGA) and the local density approximation (LDA) was applied.

1. Introduction

In recent years there has been a growing interest in alternative energies, in particular solar energy, being the research to improve efficiency and reduce costs in the manufacture of photovoltaic solar cells one of the most important ways to go. The combination of wide bandgap semiconductors and organic dyes are the main candidates in the construction of cheap hybrid solar cells. A lot of work has been done with ZnO for its opto-electrical properties, and it were found improvements in electron transport after doping it with elements of group III (Aluminum or Indium) [1]. There are a variety of doping techniques, such as implantation, but the mechanical milling has proved to be a very useful and effective one [2]. In this sense, we have previous analyzed the effects of mechanical milling on pure [3] and doped ZnO powders with a variety of doping elements [4,5]. From X-ray measurements the general observed behavior in the zincite structure was diminution of grain size as milling time increases. While for doped powders, a progressive diffraction peaks intensity diminution corresponding to the minority phase was found, indicating cation substitution at the final state of milling. This conclusion was also arrived from positron annihilation lifetime experiments [6]. Among others II–VI semiconductors, ZnSe and ZnTe have also good opto-electrical properties and may be potentially the main components for new categories of solar cells. It is important for future technological application the knowledge of defect structure of each material constituent a solar cell device. In this work we present preliminary studies of these two pure systems to establish the basis, before further

---

* *Corresponding author*. Departamento de Física Prof. Emil H. Bose, Facultad de Ciencias Exactas, Universidad Nacional de La Plata, CC 67, 1900 La Plata, Buenos Aires, Argentina. Fax: +54 221 4252006.
E-mail address: damonte@fisica.unlp.edu.ar (L.C. Damonte).

0360-3199/$ – see front matter Copyright © 2011, Hydrogen Energy Publications, LLC. Published by Elsevier Ltd. All rights reserved.
doi:10.1016/j.ijhydene.2011.12.082

doping. The structural properties on these mechanical milled powders were investigated by means of X-ray diffraction (XRD), scanning electron microscopy (SEM) and positron lifetime annihilation spectroscopy (PALS). The PALS technique has advantages respect other experimental procedures, is non-destructive and the radiation of annihilation is appropriate to investigate atomic size defects. In addition, both in metals and semiconductors, positron annihilation parameters can give useful information about density, type, size of positron capture sites.

2. Experimental procedure

Commercially powders of ZnSe (99.99%) and ZnTe (99.99%) from Aldrich Chemistry, Sigma–Aldrich Co, were milled in a steel cylinder (8 cm^3) with one steel ball (diameter 12 mm). The mechanical milling was performed in a Retsch MM2 horizontal vibratory mill during 10 h. Milled powders were compacted under uniaxial pressure of 150 MPa into disk-shaped pellets (diameter 8 mm). Starting and milled powders were characterized by X-Ray diffraction (XRD) performed with a Philips PW1710 Diffractometer with CuKα radiation in the National Diffraction Laboratory (LANADI-UNLP). Powder microstructure was also investigated by scanning electron microscopy (SEM) with a JSM6300 (JEOL Scanning Microscopy) operating at 10 kV. Positron Annihilation Lifetime measurements (PALS) were done in a conventional fast–fast coincidence system with two scintillator detectors (one BaF$_2$ and one plastic BURLE) provided a time resolution (FWHM) of 260 ps. A ^{22}NaCl (10 μCi) radioactive source deposited onto a kapton foil (1.42 g/cm^3) and sandwiched between two identical samples was used. The source contribution and the response function were evaluated from a Hf metal reference sample using the RESOLUTION code [7,8]. Positron lifetime spectra of 3 × 10^6 counts each were recorded at room temperature and analyzed with the POSITRONFIT program [7,8].

3. Results and discussion

3.1. Sample characterization

X-ray diffraction patterns for ZnSe and ZnTe powders, as received and after 10 h of mechanical milling, are shown in Fig. 1. They display the characteristic reflection lines of cubic ($F\overline{4}3m$) ZnSe and ZnTe. After 10 h of milling, a broadening of the peaks is observed as consequence of grain size reduction and internal strain induced by severe mechanical work [3].

SEM resulting images for all powder samples are shown in Fig. 2. For both semiconductors the results are quite similar. For the starting materials large and wide distribution of sizes are observed. The mechanical work process clearly changes this heterogeneity, reducing the grain size and yielding a more homogeneous powder with a certain degree of agglomeration.

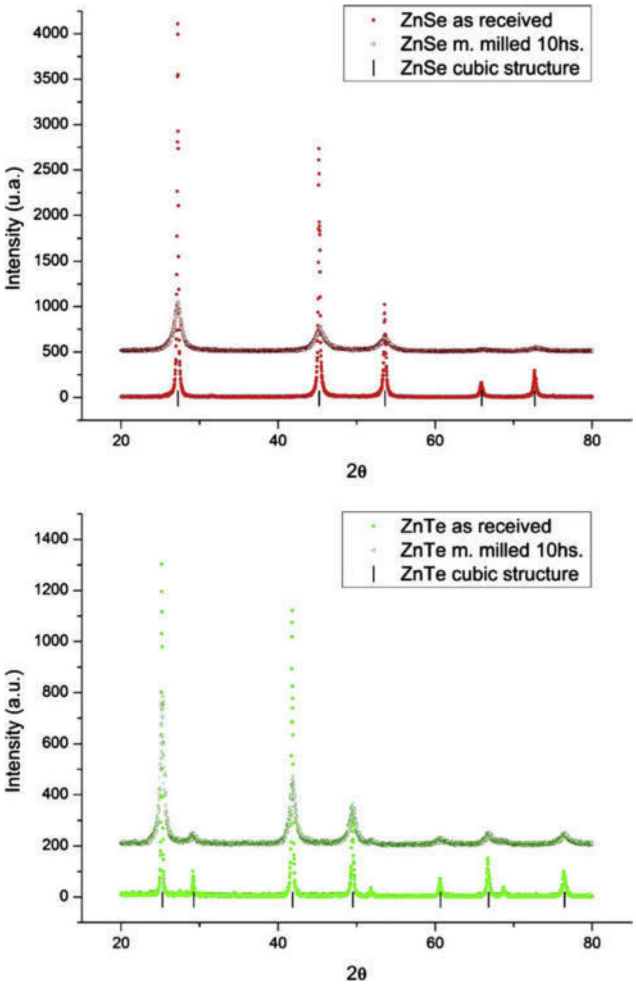

Fig. 1 – XRD patterns for ZnSe and ZnTe powders as received and after 10 h of mechanical milling. (top) ZnSe as received and after 10 h of milling; (bottom) ZnTe as received and after 10 h of milling.

Pressed unmilled and milled powders were analyzed by positron annihilation lifetime spectroscopy in order to identify the mechanically induced defects. After background and source contribution correction, the lifetime spectra for all samples

$$n(t) = \sum_i I_i e^{-t\tau_i},$$

were decomposed into two exponential decays, being each positron state characterized by a positron lifetime, τ_i, with certain intensity, I_i (normalized). The first lifetime component, associated to positron annihilation in the bulk of the material, is in agreement with reported values [9]. The second one, around 550 ps with intensities lower than 10%, take into account positron trapping at different intrinsic defect as is usually observed in semiconductor materials. During mechanical milling, the powders suffer severe plastic deformation giving rise to particle and grain refinement. Different kinds of defects, such as vacancies, vacancy clusters, dislocations, etc., are simultaneously created. This process gives place to an increase in both lifetime contributions modifying also their relative intensities. In Table 1 the resulting fitted positron parameters are shown.

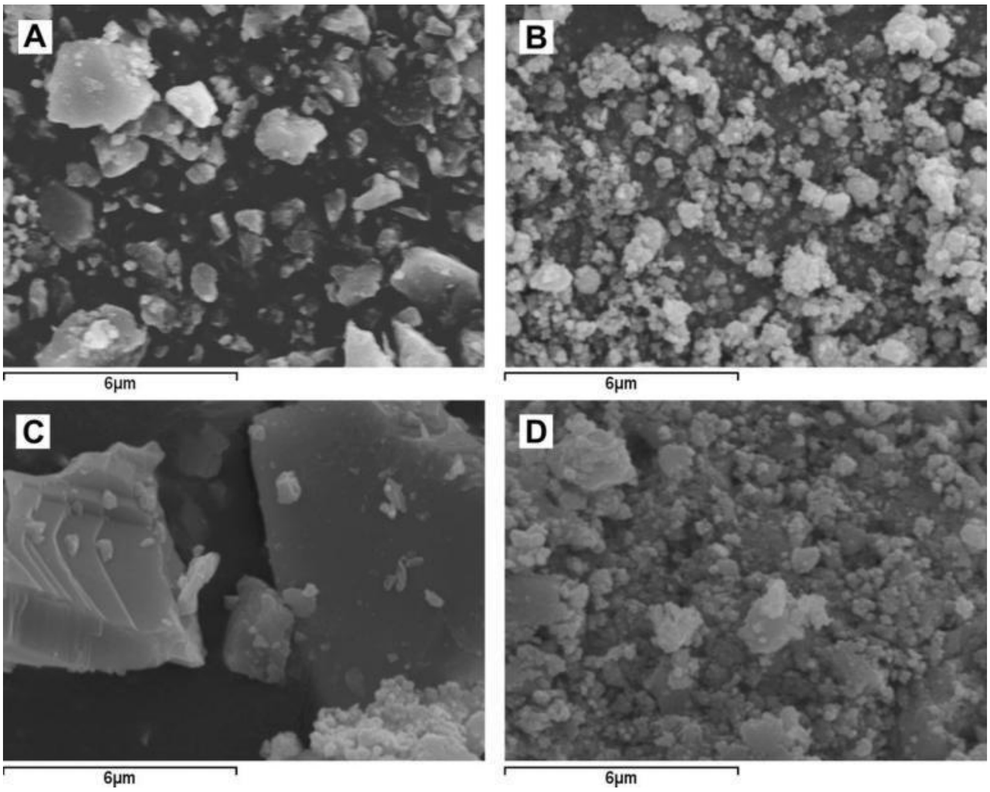

Fig. 2 – SEM micrographs of ZnSe and ZnTe powders as received and after 10 h of mechanical milling. (A) ZnSe as received; (B) ZnSe after 10 h; (C) ZnTe as received; (D) ZnTe after 10 h.

3.2. *Ab-initio calculations*

In order to obtain a better knowledge of the intrinsic and mechanical induced defects ab-initio calculation of bulk lifetime positron annihilation using the MIKA implementation were performed. This program allows to obtain the positron and electron densities working within the framework of the two-component density functional theory (TCD-FT) [10]. As it is known, the positron annihilation rate is proportional to the electronic density at the positron annihilation region and can be calculated from the overlap integral as

$$\lambda = \frac{1}{\tau} = \pi r_0^2 c \int n_+(r) n_-(r) g(0; n_+; n_-) \mathrm{d}r,$$

where r_0 is the classical electron radius, c is the speed of light, n_+ and n_- are the positron and electron densities and $g(0; n_+; n_-)$ the electron-positron pair correlation functional evaluated at the positron annihilation region. Basically, this calculation requires solving one-particle Schrödinger equations for electron and positron wavefunctions. For the positron

$$-\frac{1}{2}\nabla^2 \psi_i^+(r) + V_{eff}(r)\psi_i^+ = \varepsilon_i \psi_i^+(r),$$

where V_{eff} is the effective potential which includes three terms, a repulsive Coulomb, an exchange-correlation and a positron–electron correlation potentials. For the last two terms, being unknown, different approaches can be used. In this work, the Local Density Approximation (LDA) and Generalized Gradient Approximation (GGA) were applied for this purpose.

The final calculated lifetimes are shown in Table 1. Comparing these values with the measured lifetime τ_1 a better agreement for the LDA approximation is observed. Similar values were reported by Plazaola et al. [11] under the LDA approximation with Linear Muffin-Tin Orbital Method (LMTO-ASA) calculations for the electron and positron densities. It is known from literature that GGA approximation well described positron properties for metals materials and results less accurate for semiconductors.

Table 1 – Experimental and calculated positron annihilation lifetime parameters. τ_1 [ps], I_1 [%] are the measured lifetimes and intensities. τ_{GGA} [ps] and τ_{LDA} [ps] are the calculated lifetime with MIKA implementation using the approximations GGA and LDA, respectively.

Sample	M. Time [h]	τ_1 [ps]	I_1 [%]	τ_2 [ps]	I_2 [%]	τ_{GGA} [ps]	τ_{LDA} [ps]
ZnSe	0	221_2	67_1	530_{10}	8_1	250	233
	10	241_1	74_1	940_{50}	1_1		
ZnTe	0	235_3	66_1	560_{20}	9_1	274	254
	10	254_3	70_1	582_{30}	4_1		

4. Conclusions

Nanocrystalline ZnTe and ZnSe powders were obtained by mechanical milling. XRD and SEM measurements confirmed grain size reduction as milling proceeds. The observed trend of positron lifetimes and intensities is to increase commensurate the milling time rises, points out the formation of different kind of defects. Ab-initio calculations indicate that the LDA approximation matches better with PALS results, nonetheless, the GGA approximation shows the desired trend for both systems.

These results constitute a first step of a systematic study on these semiconductors in order to characterize their defect structure for their potential application as solar cells components.

Acknowledgments

This work was supported by the CONICET (PIP 112-200802-00128) from Argentina. Authors also acknowledge Dr. Sergio Ferrari, Dr. Marcos Meyer and Lic. Lorena Baum for their collaboration.

REFERENCES

[1] Pearton S, Norton D, Ip K, Heo Y, Steiner T. Recent progress in processing and propeties of ZnO. Progr Mater Sci 2005;50: 293–340.

[2] Suryanarayana C. Mechanical alloying and milling. Progr Mater Sci 2001;46. 1–184.

[3] Damonte L, Zélis LM, Soucase BM, Fenollosa MH. Nanoparticles of ZnO obtained by mechanical milling. Powder Technol 2004;148:15–9.

[4] Damonte L, Donderis V, Ferrari S, Orozco J, Fenollosa MH. Al-doped ZnO mechanical milled powders for dye sensitized cells. J.Alloys Compd 2010;495:432–5.

[5] Damonte L, Fenollosa MH, Meyer M, Zélis LM, Soucase BM. Structural and magnetic properties in mechanically alloyed $Zn_{1-x}Co_xO$ semiconductor powders. Physica B 2007;398:380–4.

[6] Damonte L, Donderis V, Ferrari S, Meyer M, Orozco J, Fenollosa MH. ZnO-based nanocrystalline powders with applications in hybrid photovoltaic cells. Int J Hydrogen Energy 2010;35:5834–7.

[7] Kirkegaard P, Eldrup M. A versatile program for analyzing positron lifetime spectra. Comput Phys Commun 1972;3: 240–55.

[8] Kirkegaard P, Eldrup M. Positronfit extended: a new version of a program for analyzing positron lifetime spectra. Comput Phys Commun 1974;7:401–9.

[9] Tessaro G, Mascher P. Point defect characterization of Zn- and Cd-based semiconductors using positron lifetime spectroscopy. J Crystal Growth 1999;197: 581–5.

[10] Puska M, Nieminen R. Theory of positrons in solids and on solid surfaces. Rev Mod Phys 1994;66:841–97.

[11] Plazaola F, Seitsonen A, Puska M. Positron annihilation in ii-vi compound semiconductors: theory. J Phys Condens Matter 1994;6:8809–27.